Equipping for risk: Lessons learnt from the UK shale-gas experience on assessing environmental risks for the future geoenergy use of the deep subsurface

P.L. Smedley [a],[*], G. Allen [b], B.J. Baptie [c], A.P. Fraser-Harris [d], R.S. Ward [a], R.M. Chambers [d], S.M. V. Gilfillan [d], J.A. Hall [e], A.G. Hughes [a], D.A.C. Manning [f], C.I. McDermott [d], S. Nagheli [a], J.T. Shaw [b],[i], M.J. Werner [g], F. Worrall [h]

[a] *British Geological Survey, Nicker Hill, Keyworth, Nottingham NG12 5GG, UK*
[b] *Department of Earth & Environmental Science, Simon Building, University of Manchester, Manchester M13 9PL, UK*
[c] *British Geological Survey, Lyell Centre, Research Avenue South, Edinburgh EH14 4AP, UK*
[d] *School of Geosciences, King's Buildings, University of Edinburgh, James Hutton Road, Edinburgh EH9 3FE, UK*
[e] *School of Engineering, Drummond Building, Newcastle University, Newcastle Upon Tyne NE1 7RU, UK*
[f] *School of Natural and Environmental Sciences, Newcastle University, Newcastle Upon Tyne NE1 7RU, UK*
[g] *School of Earth Sciences, University of Bristol, Wills Memorial Building, Queens Road, Clifton, Bristol BS8 1RJ, UK*
[h] *Department of Earth Sciences, Durham University, Stockton Road, Durham DH1 3LE, UK*
[i] *Now at: National Physical Laboratory, Hampton Road, Teddington, Middlesex TW11 0LW, UK*

HIGHLIGHTS

- Risks (air, water and seismic) from exploration for shale gas in UK were explored.
- Establishing baseline is critical to understanding potential environmental impacts.
- Impacts were observed for atmospheric gases, seismic response, not for groundwater.
- A combined risk-assessment framework was developed to model evolution of risks.
- Atmospheric and seismic risk is local and short-lived; groundwater is longer-term.

GRAPHICAL ABSTRACT
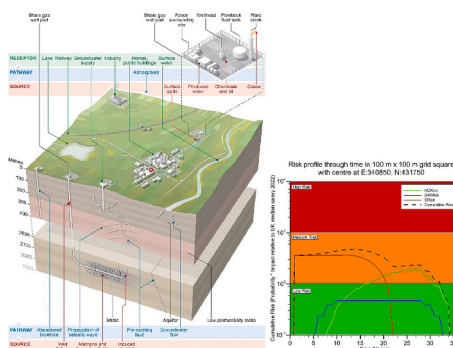
ARTICLE INFO

ABSTRACT

Summary findings are presented from an investigation to improve understanding of the environmental risks associated with developing an unconventional-hydrocarbons industry in the UK. The EQUIPT4RISK project, funded by UK Research Councils, focused on investigations around Preston New Road (PNR), Fylde, Lancashire, and Kirby Misperton Site A (KMA), North Yorkshire, where operator licences to explore for shale gas by hydraulic fracturing (HF) were issued in 2016, although exploration only took place at PNR. EQUIPT4RISK considered atmospheric (greenhouse gases, air quality), water (groundwater quality) and solid-earth (seismicity)

* Corresponding author.
  E-mail address: pls@bgs.ac.uk (P.L. Smedley).

Modelling
Risk assessment

compartments to characterise and model local conditions and environmental responses to HF activities. Risk assessment was based on the source-pathway-receptor approach. Baseline monitoring of air around the two sites characterised the variability with meteorological conditions, and isotopic signatures were able to discriminate biogenic methane (cattle) from thermogenic (natural-gas) sources. Monitoring of a post-HF nitrogen-lift (well-cleaning) operation at PNR detected the release of atmospheric emissions of methane (4.2 ± 1.4 t CH_4). Groundwater monitoring around KMA identified high baseline methane concentrations and detected ethane and propane at some locations. Dissolved methane was inferred from stable-isotopic evidence as overwhelmingly of biogenic origin. Groundwater-quality monitoring around PNR found no evidence of HF-induced impacts. Two approaches for modelling induced seismicity and associated seismic risk were developed using observations of seismicity and operational parameters from PNR in 2018 and 2019. Novel methodologies developed for monitoring include use of machine learning to identify fugitive atmospheric methane, Bayesian statistics to assess changes to groundwater quality, a seismicity forecasting model seeded by the HF-fluid injection rate and high-resolution monitoring of soil-gas methane.

The project developed a risk-assessment framework, aligned with ISO 31000 risk-management principles, to assess the theoretical combined and cumulative environmental risks from operations over time. This demonstrated the spatial and temporal evolution of risk profiles: seismic and atmospheric impacts from the shale-gas operations are modelled to be localised and short-lived, while risk to groundwater quality is longer-term.

1. Introduction

The deep subsurface is and has been increasingly a target for exploration activities in the pursuit of geoenergy developments, including in the UK. Exploration for unconventional hydrocarbons in the form of shale gas from the Carboniferous Bowland/Hodder Shale formations of north-central England has been one such activity. The last decade saw an initial increase in government interest in the development of a shale-gas industry, at least in England (Mackay and Stone, 2013; The Royal Society and the Royal Academy of Engineering, 2012), followed by a decline linked to sustained concerns over environmental, safety, technical and financial uncertainties (Baptie et al., 2022; Bradshaw et al., 2022; Bradshaw and Waite, 2017; Whitelaw et al., 2019). This was punctuated only briefly by the hydrocarbon shortages prompted by the Russian invasion of Ukraine in 2022.

In 2011, Hydraulic Fracturing[1] (HF) of the first dedicated shale-gas well in the UK, Preese Hall 1 (PH-1) near Blackpool, Lancashire, caused felt seismicity (Clarke et al., 2014) which led to the suspension of operations and initiated studies into induced seismicity and risks (The Royal Society and the Royal Academy of Engineering, 2012). The UK government published a regulatory roadmap (Department for Business Energy and Industrial Strategy, 2013) that outlined regulations for onshore shale-gas exploration in the UK with specific measures for the mitigation of HF-induced seismicity including avoiding geological faults. The roadmap included requirements to assess baseline levels of earthquake activity, monitor seismic activity during and after HF and implement a 'traffic-light' system to control decisions on whether or not injection can proceed, based on recorded seismicity. A threshold of magnitude 0.5 ML was introduced. Other regulatory controls included a requirement to disclose chemical additives to be used in HF operations. The UK Infrastructure Act (2015) also required monitoring of baseline levels of methane in groundwater for 12 months before HF could begin, as well as monitoring emissions of methane to air for the duration of the site's environmental permit.

By 2016, companies operating at two other sites in England (KMA, Yorkshire, and PNR, Lancashire) were granted licences to carry out HF for shale-gas exploration. However, in 2018, the Yorkshire site failed to obtain final government approval and so no HF activity has taken place. The Yorkshire operator's onshore business was subsequently sold and the new operator signalled a plan to direct activities away from hydrocarbon exploration. HF activity at PNR (well PNR-1z) in Lancashire was

instigated in late 2018. This was again accompanied by seismicity, with the largest event (magnitude 1.6 ML) felt by a small number of people near the epicentre (Clarke et al., 2019). HF operations in the adjacent PNR-2 well started in August 2019 and were also accompanied by seismicity, the largest of magnitude 2.9 ML (Kettley et al., 2021). The earthquake was felt up to a few kilometres from the epicentre (Edwards et al., 2021) and led to a premature end to operations, with only 7 of the planned 47 HF stages of PNR-2 completed. Following a review of these events (Oil and Gas Authority, 2019), a moratorium on shale-gas HF in England was implemented in November 2019. At the time of writing, there exists a presumption against shale-gas exploration, with moratoria on HF in place in England, Wales and Scotland, and with a similar position proposed for Northern Ireland.

In July 2018, UK Research and Innovation (UKRI), through the Natural Environment Research Council (NERC) and the Economic and Social Research Council (ESRC), funded the Unconventional Hydrocarbons in the UK Energy System programme (UKUH: http://www.ukuh.org/). The programme consisted of five research Challenge areas: (1) the evolving shale-gas landscape; (2) shale resource potential, distribution, composition, mechanical and flow properties; (3) coupled processes from reservoir to surface; (4) contaminant pathways and receptor impacts; and (5) socio-economic impacts. This study provides an overview of research findings related to the EQUIPT4RISK project (2018–2023), which addressed research Challenge 4 of the UKUH programme. The EQUIPT4RISK project was initiated at a time of growing industry momentum for shale-gas exploration in the parts of north-central England underlain by Bowland/Hodder units but ended in a very different political and economic landscape. The EQUIPT4RISK project therefore evolved and broadened to study the context of both shale gas and the wider environmental implications of deep subsurface geoenergy exploration and utilisation.

The primary aims of the project were to improve understanding and quantification of the environmental risks inherent in shale-gas development, specifically in the UK geological context. Air, groundwater and solid-earth compartments were characterised in order to understand and model their interactions and impacts. The project has also developed a risk-assessment framework to evaluate theoretical combined and cumulative risks over time from development of a shale-gas wellfield. The project has sought to improve assessment and communication of risk and to support strategies for monitoring of the environmental impacts of exploiting the deep subsurface.

2. Approach to risk assessment

The approach adopted for assessment of environmental risks is based on the established source-pathway-receptor (SPR) model concept. This is a standard tool for environmental-risk management, useful in the

---

[1] Hydraulic fracturing, commonly known as fracking, is the process of injecting water, sand, and/or chemicals into a well to break up underground bedrock to free up oil or gas reserves (www.usgs.gov/mission-areas/water-resources/science/hydraulic-fracturing)

context of shale-gas exploration for applying the concept of risk to air quality and atmospheric emissions, groundwater quality and ground motion, including seismicity. The source constitutes the activity posing the environmental threat (deep gases, formation fluid, well failure, seismic events and site activities), the receptor the environmental target (s) at risk (e.g. air, drinking water, ecosystems, infrastructure and populations) and the pathway the route and/or processes between sources and receptors. The various identified sources, pathways and receptors in the context of shale-gas-exploration risk are outlined in Fig. 1.

2.1. Risks for air quality and greenhouse-gas emissions

The risks related to the atmosphere primarily involve emission of pollutants during different phases of shale-gas site operations. Potential air pollutants can be separated into two broad categories, with risks distributed across different spatial and temporal scales. The first

category includes pollutants that impact directly upon air quality, thereby posing risks to both human and environmental health. Any potential risk is typically expected to be highly localised and is usually restricted to receptors in close proximity (<1 km) to onsite sources. This risk typically diminishes sharply with distance due to atmospheric dispersal. Pollutants within this first category include both primary and secondary sources. Primary pollutants are those emitted directly by operations, and may include carbon monoxide (CO), nitrogen oxides (NO_x), non-methane hydrocarbons (NMHCs), and particulate matter (PM) such as black carbon (BC) and organic carbon (OC). Such pollutants are typically emitted from combustion sources onsite (e.g. diesel generators and gas flaring) and specific activities that may loft pollutants (e.g. truck movements) (Orak et al., 2021). Secondary pollutants are created through chemical processing of primary emissions as they mix and advect in the atmosphere and may include nitrogen dioxide (NO_2) and ozone (O_3). The potential health impacts of many of these
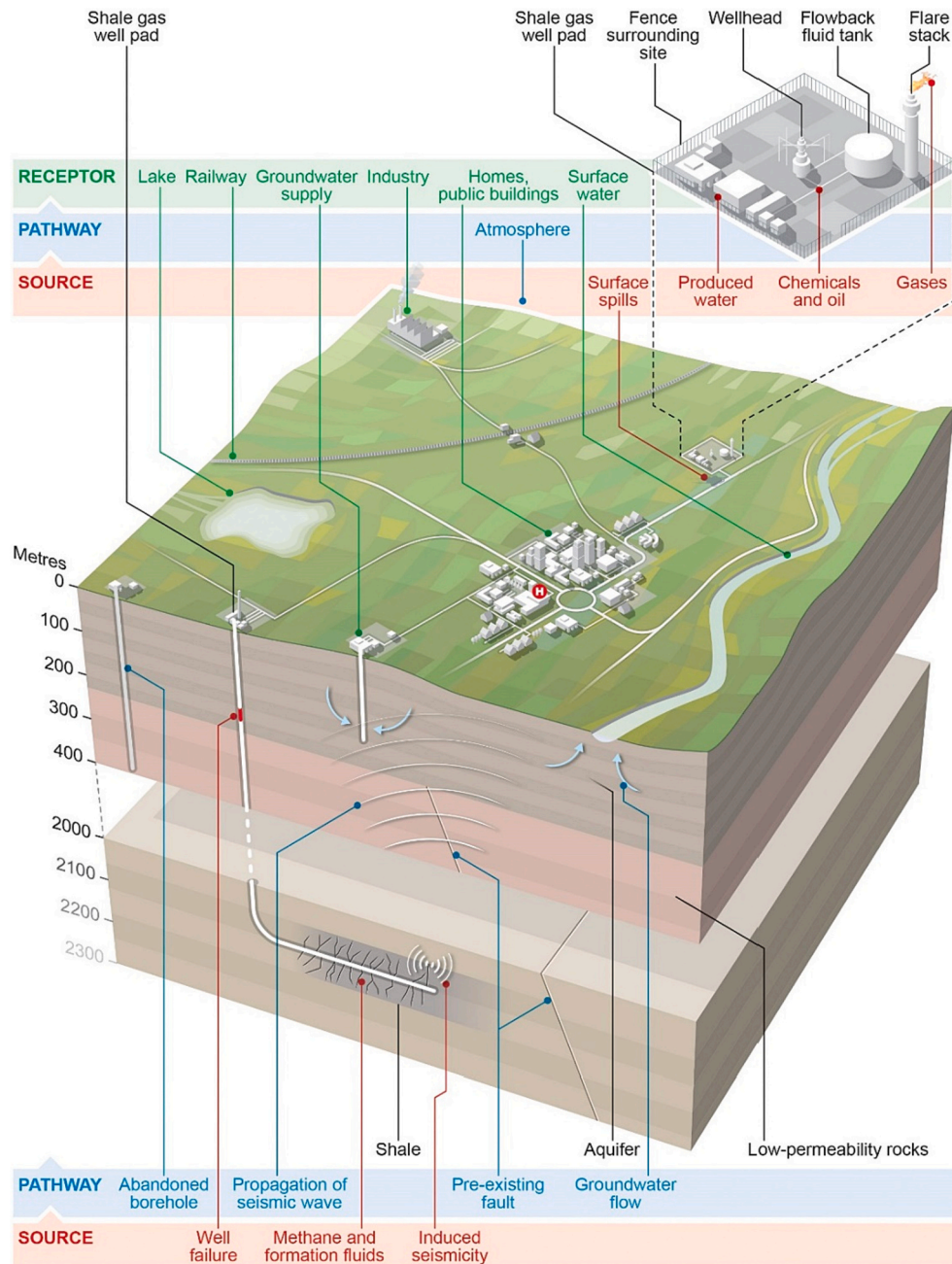

Fig. 1. The source-pathway-receptor approach to assessing risk in the context of shale-gas exploration.

pollutants are well known and typical of urbanised/industrial development and therefore they are routinely monitored at sites nationally and globally, with regulations in place to limit acute and chronic human exposure.

High concentrations of NMHCs, including potentially carcinogenic aromatic compounds, were detected multiple times downwind of a refractured well pad in the Uintah Basin, central USA (Warneke et al., 2014). Such NMHC detections, coupled with local NO_x emissions, have led to unusual and extreme production of O_3 in winter in urban areas, with O_3 concentrations well in excess of contemporary air-quality standards (Edwards et al., 2014). Elevated concentrations of particulate matter (PM2.5) have also been associated with HF and unconventional shale-gas extraction (Walters et al., 2015).

The second category of pollutants associated with shale-gas operations includes those that present a risk to climate change. This risk relates to a larger spatial scale (national and global) and can also be considered over lengthier time scales due to the persistence of some components in the atmosphere for multiple decades or longer. This category of pollutants includes carbon dioxide (CO_2), with an atmospheric lifetime of up to 1000 years, and shorter-lived climate pollutants (SLCPs) such as methane (CH_4). BC and O_3 are also categorised as SLCPs, and some chemical species can therefore be considered a risk to both air quality and human health, as well as to longer-term climate change. Climate impacts from this category of pollutants can be considered a risk to the success of international obligations, such as the Paris Agreement, or to national policies, such as Net Zero (Nisbet et al., 2020; Nisbet et al., 2019).

Examples of CO_2 and CH_4 emissions that can be associated directly with HF are difficult to find, largely because fossil-fuel basins in the USA host operations from a combination of conventional and unconventional sources. Lifecycle assessments of shale gas extracted via HF have been controversial, with differing opinions on the carbon footprint relative to conventionally extracted shale gas, liquefied natural gas, coal and oil (Howarth, 2015; Jenner and Lamadrid, 2013; Mackay and Stone, 2013). Generally, the carbon footprint is assessed based on the time horizon over which impacts are considered and the magnitude of CH_4 leakages along the supply chain, with leak rates of between 1 % and 4 % altering the shale-gas footprint relative to other fuels (Allen, 2014; Alvarez et al., 2012). Emission inventories provide estimates associated with operations and activities but are often based on historical data and outdated practices (Allen, 2014). The range in emissions from the same type of activity can also be huge: Allen et al. (2013) measured CH_4 emissions of between 0.01 Mg and 17 Mg (average 1.7 Mg) across 27 hydraulically fractured well completions in the USA. This contrasts with the US EPA greenhouse-gas inventory (for 2011), which estimated emissions from well completions on average at 81 Mg of CH_4 (Allen, 2014).

2.2. Risks to groundwater quality

Risks to groundwater quality from a developing shale-gas industry include potential impacts from surface spillages of HF fluid and any surface-stored flowback fluid returned from depth. Potential hazards include any chemical compounds added to the frack fluid for improved operation, and salinity and naturally-occurring radioactive materials (NORM) (notably ^{226}Ra and ^{222}Rn gas) present in flowback. These fluids contained at surface could potentially infiltrate a shallow aquifer depending on its permeability and flow paths and risks are covered by existing well-established risk assessments and regulation for surface-borne chemical contamination. Potential risks also include contamination of shallow groundwater via deep subsurface pathways, either from the shale source itself via induced fractures, via existing potentially rejuvenated faults, via failed borehole casings with either existing weaknesses or through damage caused during operations, or via old disused hydrocarbon boreholes. Risks of solute contamination of receptors from these subsurface pathways include dissolved gases (notably CH_4, higher alkanes, CO_2) as well as the same salinity and NORM

hazards inherent with surface-stored flowback fluids. Deep subsurface flow pathways are typically long (shale source-rock depths >1500 m deep) and pathways invariably through deep, indurated and largely low-permeability sedimentary rocks.

Some occurrences of hydrocarbon gases in shallow groundwater in the USA have been inferred to derive from deep shale-gas sources associated with HF (Osborn et al., 2011) although the evidence has been contested (Molofsky et al., 2013). Migration of CH_4 from deep sources has most commonly been attributed to preferential flow caused by poor integrity of production-well casings (Hammond et al., 2020; Osborn et al., 2011). Occurrences of organic compounds found in HF fluid have also been reported in shallow drinking-water wells but again, sources and pathways of the contaminants have not been established unequivocally (Llewellyn et al., 2015).

2.3. Seismic risks

Over the last decade, the number of observations of induced seismicity caused by HF operations around the world has increased as the shale-gas industry has developed (Atkinson et al., 2020). Although induced earthquakes large enough to be felt by people are relatively rare (Atkinson et al., 2016), some regions appear to be more susceptible (Schultz et al., 2018). There are also examples of earthquakes induced by HF operations large enough to have been felt widely, or even to have caused damage. For example, a magnitude 3.9 Mw earthquake was associated with operations in the Duvernay Formation in the Alberta Basin of Canada in 2015 (Schultz et al., 2015; Schultz et al., 2017). In 2015, a magnitude 4.6 Mw earthquake occurred during operations in the Montney Formation that spans the border between British Columbia and Alberta in western Canada (Babaie Mahani et al., 2019; Babaie Mahani et al., 2017). A magnitude 4.0 Mw earthquake in the Eagle Ford Shale play in South Texas in 2018 is the largest HF-induced earthquake documented in the USA (Fasola et al., 2019). The largest documented example of an earthquake induced by HF operations to date is a magnitude 5.7 ML earthquake in the Sichuan Basin of China in 2018 (Lei et al., 2019) that caused approximately $7 M US in direct economic losses alongside human fatalities and injuries.

Widely-used probabilistic methods to assess hazards and risks for tectonic earthquakes (see Baker et al., 2021 for a comprehensive treatment of this subject) can also be applied to induced seismicity, with suitable adjustments. The risk at a given site is generally considered to be a function of the size of a possible earthquake, the distance of the site from the location of the earthquake, local ground conditions, and the vulnerability of any buildings or structures at the site. The hazard for different earthquake scenarios can be evaluated using an empirical ground-motion prediction equation (GMPE), a formula that predicts the amplitude of earthquake ground motion based on factors such as magnitude, distance, depth and site amplification (Bommer, 2022). Damage to surface structures due to earthquake shaking is the result of inertial forces, causing the centre of gravity of the building to move relative to its base or foundation. The estimated ground-motion hazards can then be translated into a risk metric, such as damage impacts using fragility functions that predict damage to components or structures (e.g. Korswagen et al., 2019). The severity of risk is then determined using an exposure model.

3. Materials and methods

3.1. Atmospheric composition

A baseline climatology of atmospheric composition was established well ahead of HF exploration to facilitate a comparative assessment of local impact associated with the lifecycle of HF well-pad operations. Analogous measurements were continued throughout exploration and for a period of one year following closure of both the PNR and KMA sites. Typically, this direct comparative approach has not been possible at

other international shale-gas sites. To this end, a fixed-site outdoor atmospheric monitoring station was established in 2014 approximately 400 m to the east of the PNR site, with a second equivalent station established in 2016 on the fenceline boundary of the KMA site (Fig. 2). Each monitoring site collected high-precision calibrated in-situ measurements of key air pollutants, greenhouse-gas concentrations and thermodynamics (pressure, temperature, winds and specific humidity). Real-time atmospheric composition measurements included nitrogen oxides (NO_x), ozone (O_3), hydrogen sulphide (H_2S), methane (CH_4), carbon dioxide (CO_2) and particulate matter (PM).

All in-situ measurements were sampled every second (frequency of 1 Hz) and averaged to 1-min periods for analysis. Whole air samples were also taken at weekly intervals for offline (laboratory) analysis of volatile organic compounds (VOCs), non-methane hydrocarbons (NMHCs), and the isotopic fraction of ^{13}C in CH_4 ($\delta^{13}C$-CH_4) to aid source apportionment. A statistical climatology, consisting of mean, median, standard deviation and percentile concentrations for each species was developed and analysed temporally for time-of-day, day-of-week, monthly, seasonal and interannual patterns and trends for each pollutant. Correlations with wind direction and airmass history were also analysed to study the relative influences of extant local and regional emission sources extraneous to the shale-gas site. This suite of measurements and the climatological baseline approach was targeted to the pollutants of interest associated with shale-gas activities based on US experience. For example, NO_x and PM emissions have been associated with diesel generators and lorry movements, while CH_4 is of particular interest as a
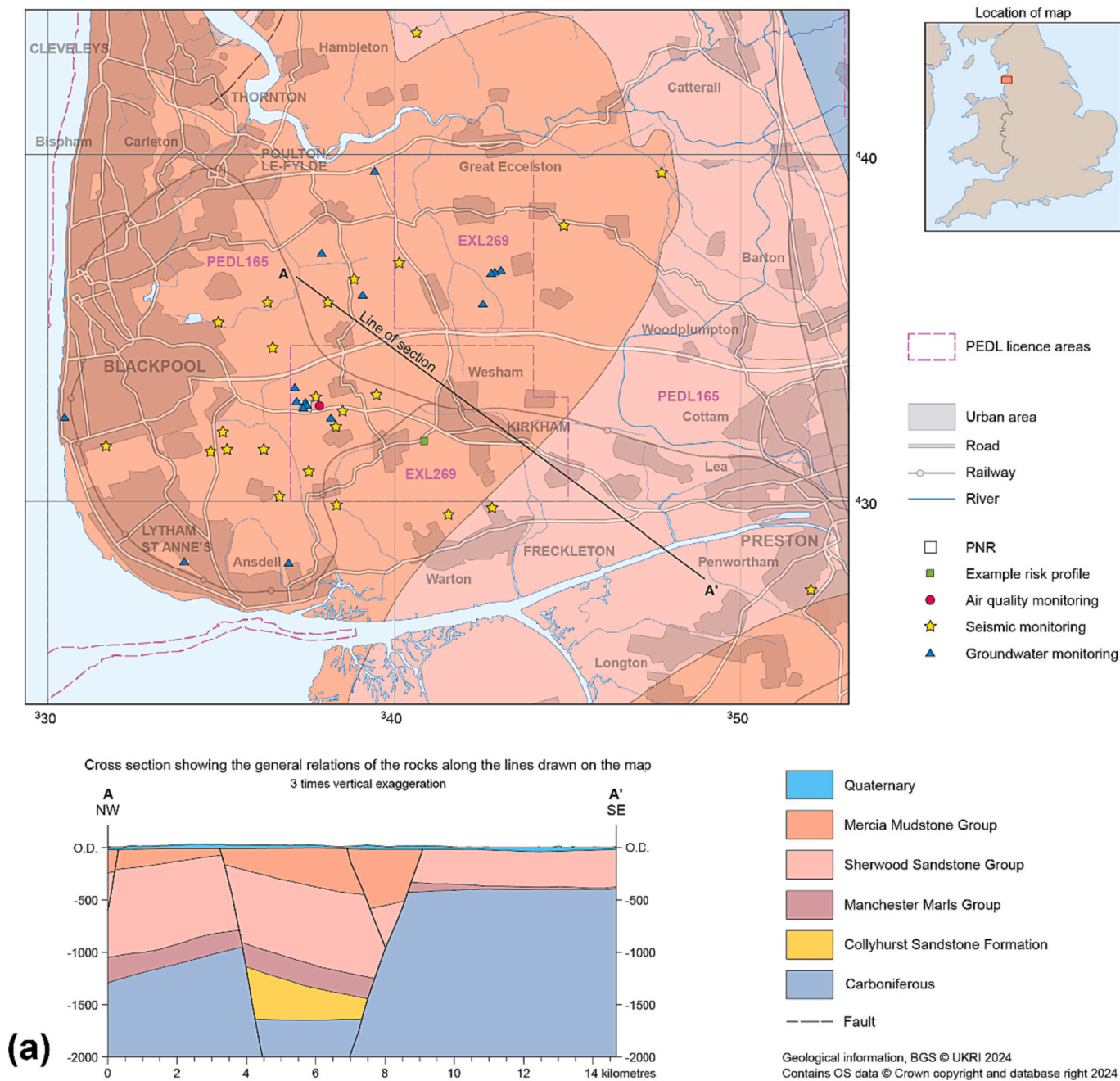

Fig. 2. Geological maps and cross sections of the (a) Lancashire and (b) Yorkshire study areas with locations of PNR and KMA well pads, air, groundwater and seismic monitoring sites and the example risk-profile location for Lancashire (see Section 4.5). Groundwater monitoring sites comprise those abstracting from Quaternary deposits in Lancashire and from Quaternary/Kimmeridge Clay Formation deposits in Yorkshire. The Bowland Shale target for shale-gas extraction lies within the Carboniferous strata.
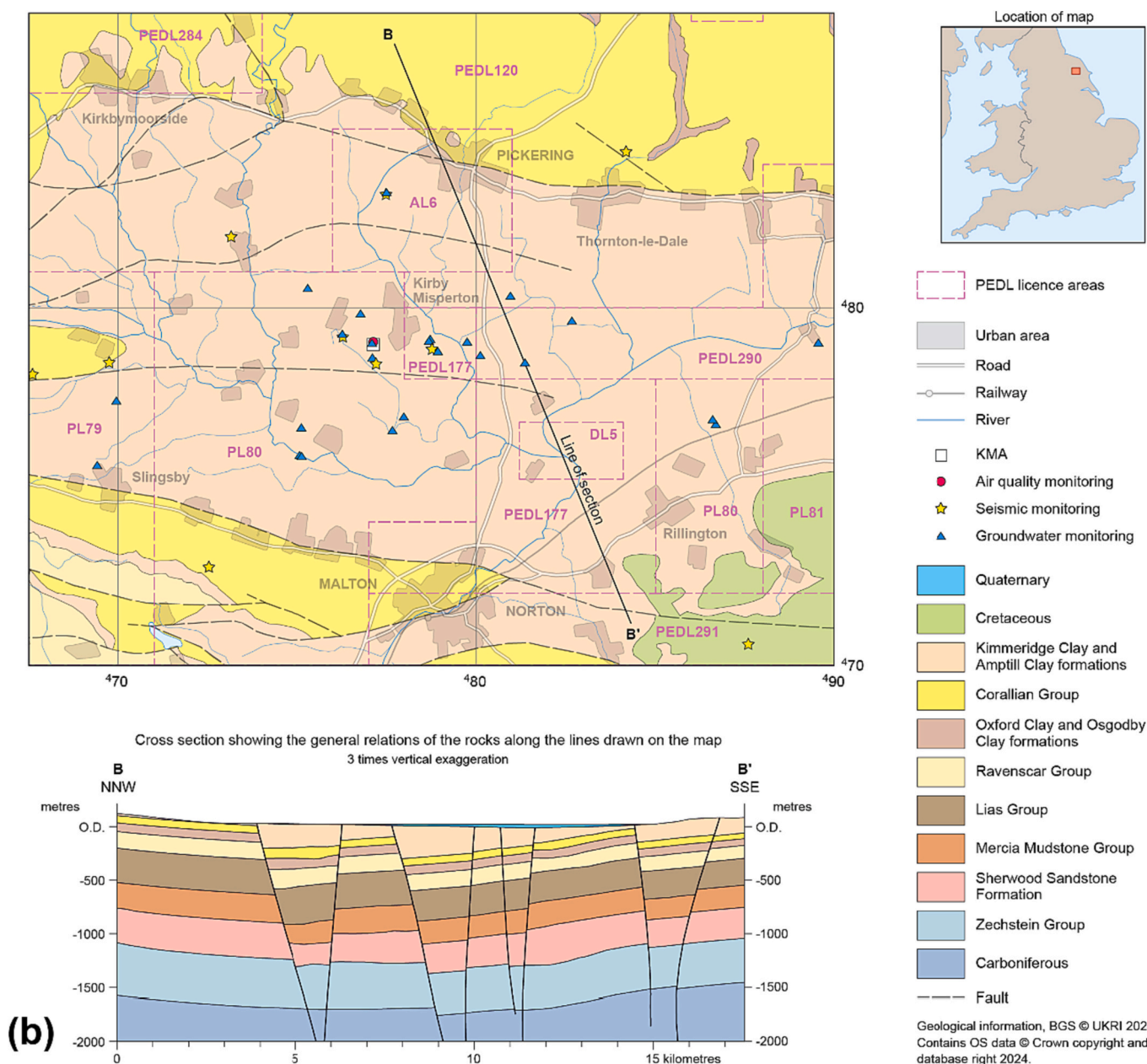
Fig. 2. (*continued*).

short-lived potent greenhouse gas with potential for fugitive emissions (defined as non-point emissions with multiple sources). By establishing the above climatology prior to exploration, it was possible to discern and quantify the incremental impact of shale-gas activities and comparison of this to existing sources of pollution in both areas.

The siting of the PNR monitoring station was east of the PNR shale-gas site (see Fig. 2) in order to take advantage of the predominant westerly winds in this coastal area and the relatively clean maritime inflow upwind to the west. The 400 m distance from the HF site was to allow any emissions to mix such that monitoring-station instrumentation had a greater chance of detecting the presence of emissions generally, and for quantifying concentrations analogous to those of exposed populations in the immediate vicinity. Suitable off-site locations were not available for the KMA site, requiring the fenceline siting. For a full description of the site design and instrumentation, and discussion of the baseline climatology of atmospheric composition prior to HF exploration, see Shaw et al. (2019) and Purvis et al. (2019) for greenhouse gases and air quality respectively. A summary of the

activities related to atmospheric composition is also given in Table 1.

In addition to continuous fixed-site measurements, case studies were made at targeted times in the lifecycle of the HF exploration sites to provide more granular atmospheric-composition data. This included spatial mapping between 2016 and 2020, using a vehicle-based mobile laboratory measuring CH_4, CO_2 and C_2H_6 at 1 Hz (Lowry et al., 2020), as well as unmanned aerial vehicle (UAV) surveys (Shah et al., 2019; Shah et al., 2020b), and site walkover surveys. Machine-learning approaches were also developed to automate the detection of CH_4-emission events using baseline data as priors for training (Shaw et al., 2022). Typically, such case studies were designed for (or responded to) onsite events such as the initiation of drilling, flowback operations, or detection of significant methane emissions associated with unignited flares. In such circumstances, targeted spatial sampling enabled the quantification of emission fluxes (mass emission rate), thus complementing the detection capabilities of fixed-site monitoring.

Table 1

Summary of approaches to assessing sources, pathways and receptors in the EQUIPT4RISK project, with outputs and links to project data.

Compartment	Baseline	Source	Pathway	Receptor	Partners	Data source
Atmospheric greenhouse gases and air quality	Statistical climatology Mobile surveys Extant sources	Site lifecycle activities Acute fugitive emissions Extraneous sources	Airmass history analysis Chemical transport modelling Gaussian plume modelling Faults, well integrity Diffuse fugitive gases	Population density Fixed-site monitoring Global atmosphere	UM, RHUL, UDur, UEdin with UYork	CEDA; NGDC; Github; (Lowry et al., 2020); Shah et al. (2019); Shah et al. (2020b); Shaw et al. (2019); Shaw et al. (2021); Shaw et al. (2022); Wilde et al. (2023)
Groundwater and aquifer gases	Groundwater-chemistry baseline monitoring, including real-time Hydrocarbon gases	Solute escape via fractures in overburden Flow via fracks Well-integrity failure; Surface spills	Particle tracking based on flowpaths Groundwater modelling	Aquifer abstractions Baseflow to surface water Groundwater-dependent wetlands Groundwater quality	BGS, UEdin	https://www2.bgs.ac.uk/groundwater/shaleGas/monitoring/lancashire.html; https://www2.bgs.ac.uk/groundwater/shaleGas/monitoring/yorkshire.html; Smedley et al. (2023)
Solid-earth seismicity	National-scale model capturing probability of ground shaking from background tectonic earthquakes (Mosca et al., 2022)	Deterministic model relating injected volume to cumulative seismic moment and earthquake magnitudes (Cremen and Werner, 2020) Statistical ETAS models with stationary and non-stationary background rates (Mancini et al., 2021)	Empirical ground-motion prediction model calibrated using PNR data (Cremen et al., 2019)	Building data from Ordnance Survey (OS) mapping, accessed through Edina Digimap (Morris et al., 2000) Building footprint information: "Buildings" layer of the OS VectorMap Local product Building height information from OS MasterMap "Building Height Attribute" database	BGS, UBris	Homogenised catalogues of microseismicity and pumping data from PNR-1z and PNR-2 injection wells used by Mancini et al. (2021), available at the National Geoscience Data Centre: doi:https://doi.org/10.5285/856fc9f4-bea8-490f-b709-92549d692da4. Dataset available under Open Government Licence; Kettlety and Butcher (2022)

UM: University of Manchester; RHUL: Royal Holloway University of London; UDur: University of Durham; UEdin: University of Edinburgh; UBris: University of Bristol; UYork: University of York; BGS: British Geological Survey.

3.2. Groundwater quality and flow

The groundwater components of the project investigated potential pathways of contaminants from deep hydrocarbon exploration around PNR and KM. Groundwater quality was investigated by the initiation of monitoring programmes involving a network of third-party and newly-drilled boreholes at each location. In Fylde, shallow groundwater is abstracted from Quaternary superficial fluvioglacial deposits in the area around PNR, although further east (Fig. 2a), Sherwood Sandstone Group strata are upfaulted and occur at shallow depth below Quaternary deposits and are used for groundwater abstraction. A borehole network was set up, penetrating the Quaternary superficial deposits (to depths of around ≤40 m). This consisted of 17 third-party boreholes and 11 newly-drilled boreholes (Fig. 2a) (Smedley et al., 2022; Ward et al., 2018a). Monitoring of a further 9 third-party boreholes in the Sherwood Sandstone Group was carried out for other projects. In the Vale of Pickering, shallow aquifers (≤60 m depth) comprise minor Quaternary superficial glaciolacustrine deposits and Jurassic Kimmeridge Clay Formation and Corallian Group strata. Some deeper boreholes (to 180 m in the Kimmeridge Clay Formation and to 227 m in the Corallian Group) were also included in the network. The network comprised 30 third-party boreholes and 14 newly-drilled boreholes (Fig. 2b) (Smedley et al., 2023; Smedley et al., 2015; Ward et al., 2020).

As ultimately no shale-gas exploration took place at KMA, the Vale of Pickering study is restricted to a robust baseline characterisation. Investigations at both locations focused on characterisation of the groundwater baseline in terms of its chemical (major and minor ions, trace elements, dissolved gases (CH_4, C_2H_6, CO_2) and selected organic compounds: polycyclic aromatic hydrocarbons, volatile and semi-volatile organic compounds, total petroleum hydrocarbons, acrylamide) and stable-isotopic ($\delta^{13}C\text{-}CH_4$, $\delta^2H\text{-}CH_4$) composition and on monitoring of groundwater chemical variability over time. Monitoring intervals varied mostly between monthly and quarterly. Data for

groundwater chemistry were acquired for both study areas via several projects including EQUIPT4RISK over the period 2015–2022. Methodology for groundwater sampling and analysis is provided elsewhere (Smedley et al., 2023; Smedley et al., 2015; Ward et al., 2020).

To provide the pathways for input into the integrated risk assessment, a groundwater-flow model for Fylde was created based around PNR as this had the most well-developed models for other categories of risk. The MODFLOW model was developed alongside a MODPATH model to provide particle tracking (advective transport only) to feed into the risk-integration activities. The model is driven by recharge derived from the national recharge model, developed using the code ZOODRM (Mansour et al., 2018), and the basis of the groundwater-flow model, cookie-cut from the British Groundwater Model, BGWM, and uses the MODFLOW6 code (Bianchi et al., 2024). The boundaries were taken as the coast to the west of Fylde (fixed head of 0 m above OD) and rivers, including the Ribble Estuary. The model was built to 400 m below ground level and consists of three layers used to represent from base, the Sherwood Sandstone Group, Mercia Mudstone Group, and overlying Quaternary deposits. A steady-state groundwater-flow model was created to obtain the velocity field to run MODPATH which was used to create particle tracks. These particle tracks were combined with chloride (Cl) concentrations and the data processed to provide the pathways to feed into the SPR model for the risk-integration process. Other conservative elements such as bromine (Br) could have been used for the process but, while Br concentrations were available, Cl was used for simplicity.

3.3. Seismicity

Networks of surface seismometers were installed to monitor background seismicity in both the Vale of Pickering and Fylde. The Vale of Pickering network consisted of seven near-surface sensors and four sensors installed in shallow boreholes. In Fylde, surface sensors were

deployed at distances of 1.5 to 20 km from the surface position of the PNR-1z well, by Cuadrilla Resources Ltd. (the operator), the British Geological Survey (BGS) and the University of Liverpool.

Continuous data from all the surface sensors were used to detect seismic events in near real-time using a short-term-average/long-term-average algorithm (e.g. Johnson et al., 1995). This approach yielded a total of 188 events detected on a minimum of three surface sensors during operations in the PNR-1z well in 2018. The largest of these had a magnitude of 1.6 ML (Clarke et al., 2019). The same approach was used to detect 260 events during operations in the PNR-2 well in 2019. The largest of these had a magnitude of 2.9 ML (Edwards et al., 2021; Kettlety et al., 2021).

Seismicity during operations in the PNR-1z well was also recorded by the operators with a downhole geophone array in the adjacent PNR-2 well. Similarly, seismicity during operations in the PNR-2 well was recorded by a downhole geophone array in the adjacent PNR-1z well. In each case, the downhole array consisted of 12 three-component geophone tools. The geophones recorded almost continuously from the onset of operations in each well, detecting over 38,000 microseismic events from PNR-1z and over 55,000 events from PNR-2 (Clarke et al., 2019; Kettlety et al., 2021).

A combined catalogue of seismic events recorded during PNR HF operations was prepared by Kettlety and Butcher (2022) (Table 1), informed by the analysis and magnitude-scaling relations developed by Baptie et al. (2020). Pumping data during operations at PNR-1z and PNR-2, including both injected volume and injection rate data originally made available by the operator and the Oil and Gas Authority has been published by Cuadrilla Resources and British Geological Survey (2021) (Table 1).

Our approach to evaluating the risks from induced seismicity can be divided into three main parts: 1) earthquake forecast models that capture the spatial and temporal variation of earthquakes of different magnitudes during and after operations; 2) estimating the resulting ground motions for events of different magnitudes in terms of specific measures of seismic intensity, and 3) integrating these along with models of exposure to calculate the resulting seismic risks. This follows the source-pathway-receptor approach that can be scaled to multiple operations across specific regions of interest. In addition, we investigated the physical mechanisms leading to the induced seismicity at PNR and analogues elsewhere (e.g. Holmgren et al., 2023; Kettlety et al., 2020; Kettlety et al., 2019).

We explored two possible forecast models, which were both linked to the volume of fluid injected during operations, that were calibrated and tested using the data from PNR. Firstly, Cremen and Werner (2020) developed a framework for assessing seismic risk by combining an injection-volume-based statistical model of event magnitudes (Hallo et al., 2014) with a ground motion prediction equation (Cremen et al., 2020; Cremen et al., 2019), and an exposure model for nearby buildings. The model relates the cumulative seismic moment release to injected volume using a scaling parameter called the seismic efficiency, which was then combined with the Gutenberg-Richter law to estimate the magnitude of the largest induced earthquake. This links quantitatively the volume of fluid injected with the potential for nuisance felt ground motions.

Secondly, Mancini et al. (2021) used an epidemic-type aftershock sequence (ETAS) approach (Ogata, 1988), a statistical model originally developed for tectonic sequences, to model the induced seismicity during HF operations at PNR. These included both a standard tectonic ETAS model where seismic rate is given by a time-independent background rate plus a function accounting for the history of triggering contributions from all previous events, and non-standard ETAS models where either averaged or sleeve-specific fluid-injection parameters are used to determine non-stationary background rates. In addition, the average response to injection observed at PNR-1z was used to make an out-of-sample forecast of the PNR-2 seismicity.

Cremen et al. (2019) and Cremen et al. (2020) developed an empirical ground-motion prediction equation specifically designed for HF-induced seismicity in the UK. This provides a median prediction of the intensity of the ground motion in terms of moment magnitude, a measure of the size of the induced earthquake, and the distance to a specific site of interest, that is used to quantify possible impacts on buildings and people. The form of the empirical model is based on a model for geothermal-induced seismicity (Douglas et al., 2013), which was modified using observed data from both PNR and from mining-induced seismicity (Verdon et al., 2017) to improve its applicability to HF-induced seismicity. The model includes both inter-event and intra-event standard deviations that capture the variability of possible earthquake ground motions. Holmgren and Werner (2021) also evaluated the new model against observed ground motions from seismic events induced by the United Downs Deep Geothermal Power Project, Cornwall, UK.

3.4. Risk integration

Potential approaches developed to assess risks from shale-gas development include multi-hazard risk assessments based on the bow-tie approach (e.g. Garcia-Aristizabal et al., 2019), specific environmental/ecosystem assessments e.g. surface waters (Maloney et al., 2018), or novel assessment methodologies for induced seismicity e.g. nuisance risk and traffic-light protocols (Cremen and Werner, 2020; Schultz et al., 2021). However, these approaches cannot provide a holistic assessment of the spatial and temporal cumulative effects and associated risk as subsurface geoenergy applications are developed. We therefore developed a cumulative-risk modelling approach for the different environmental compartments based on the Integrated Assessment Model (IAM) approach. IAMs typically comprise a collection of low-fidelity models, also known as Reduced-Order Models (ROMs), that derive from complex high-fidelity models of individual components of a system. These allow for whole-system assessment via the integration of the sub-system ROMs e.g., NRAP-IAM-CS (Pawar et al., 2016; Vasylkivska et al., 2021). This approach has previously been proposed as a method to assess engineering risk in the US shale-gas industry based on a features, events and processes framework (Soeder et al., 2014).

We aimed to develop a framework to provide a cumulative risk assessment, combining potential hazards from the three main environmental compartments: air, water, and solid earth (seismicity). The framework, based on the SPR approach, is designed to enable an assessment of how the cumulative risk evolves both in space and time as a shale-gas play may develop. The outcome is a methodology that captures a more holistic view of the environmental and infrastructure risk through time, which is also appropriate for multiple future subsurface applications.

3.4.1. The framework

The outputs of the characterisation and modelling studies conducted in the air, water or seismicity compartments provide fundamental data and tools for integrated risk modelling. The main goal was to estimate the cumulative risk from subsurface operations on sensitive human, environmental and infrastructure receptors and to define how the risk changes over temporal scales (i.e. lifetime of a prospective resource development: HF, production, well abandonment) and spatial scales (e.g. multiple well pads, multiple receptors). The spatial extent of the implementation was based on the UK Government's Petroleum Exploration and Development Licence (PEDL) 165 area covering PNR and the potential impact on the wider area of Fylde, Lancashire (see Fig. 2).

Ensuring that each potential hazard is assessed with respect to a common metric is critical to being able to compare the risk from different hazard sources. 'Risk' is often defined as the likelihood of an event occurring multiplied by its impact (Kasperson and Kasperson, 2001). Within the SPR approach, the likelihood refers to the probability of an event occurring that provides a source of a given magnitude, for example, emission of a pollutant, contaminant spill or induced seismic

event. Whether the source has an impact is then a function of the pathway from the source to a receptor. The presence and sensitivity of the receptor to a particular source defines its vulnerability which is computed with value of the consequence of the event to determine the impact.

A key tenet of the framework was to ensure that it can be embedded in the ISO 31000 Risk Management Framework to allow for a continual feedback loop for monitoring and mitigation. Fig. 3 shows the workflow for the risk-assessment methodology and the considerations included in the model framework, indicating how each hazard is combined with the chosen receptors.

3.4.2. Source-pathway modelling

The high-fidelity models from which the ROMs were developed comprise a Gaussian Plume air-quality model (Connolly, 2019; Shaw et al., 2020), groundwater flow and particle tracking based on the BGWM (Bianchi et al., 2024), and the nuisance seismic-risk model developed by Cremen and Werner (2020). The ROMs represent the pathway, while the source locations and magnitudes are defined by the user based on the location of the proposed (or existing) well pads, and the receptors are captured within the user-defined receptor model.

Each ROM generates a spatial-temporal distribution of the probability of exceeding a pre-defined impact threshold, based on multiple stochastic realisations of different source magnitudes. The framework is designed so that the ROMs for each physical system produce output of the same format. To do so, a common metric of the probability of exceeding a given threshold is defined. The threshold is user-defined and relates to the hazard magnitude that results in a calculable impact at the receptor. The probability of exceedance of each hazard can then be combined as a union or intersection to give the combined probability of exceeding one, some, or all, impact thresholds, i.e. disaggregated or cumulative impact.

Multiple well pads are simulated on a licence domain with air-pollutant concentrations calculated from an annual reference plume,

groundwater contaminant concentration calculated from a 1D conservative-transport analytical model along stream traces using chloride (Cl) ions and release functions based on US well leak data from Davies et al. (2014), and peak ground velocities determined from a reference seismicity distribution.

3.4.3. Receptor impact modelling

A receptor model captures different categories of receptors for each hazard compartment and facilitates the combination of receptors where vulnerability overlaps e.g., population and buildings, using a 100 m × 100 m grid. Impact models specific to the receptor calculate the economic cost of exceeding the impact threshold, normalised to the average annual salary of the UK, which can then be combined based on the methodology of combining the probabilities.

In this initial demonstration of the framework, the atmospheric risk is focused on the air-quality impact and its spatial and temporal evolution on the scale of a licence area. While the approach therefore does not consider the risk posed through any contribution to climate change it enables the atmospheric risk to be compared directly with the risk from groundwater contamination and/or induced seismicity. Future iterations of the framework could include the wider impact on climate change.

Air-quality impacts are modelled using lifetables based on the long-term impact of increments of 10 $\mu g/m^3$ increase in NO_x and PM, following the COMEAP (2010); (COMEAP, 2018) and impact assessment approach (UK Govt, 2023). The number of life years lost per person is translated into an economic cost using this framework and is used to ascertain the total economic impact per grid square based on the population density.

Groundwater impacts are calculated based on the economic cost of blending contaminated water with groundwater until the contaminated water is below the regulatory threshold (the national drinking-water standard). The required groundwater abstraction rate is calculated and used with the net present value of groundwater to determine the
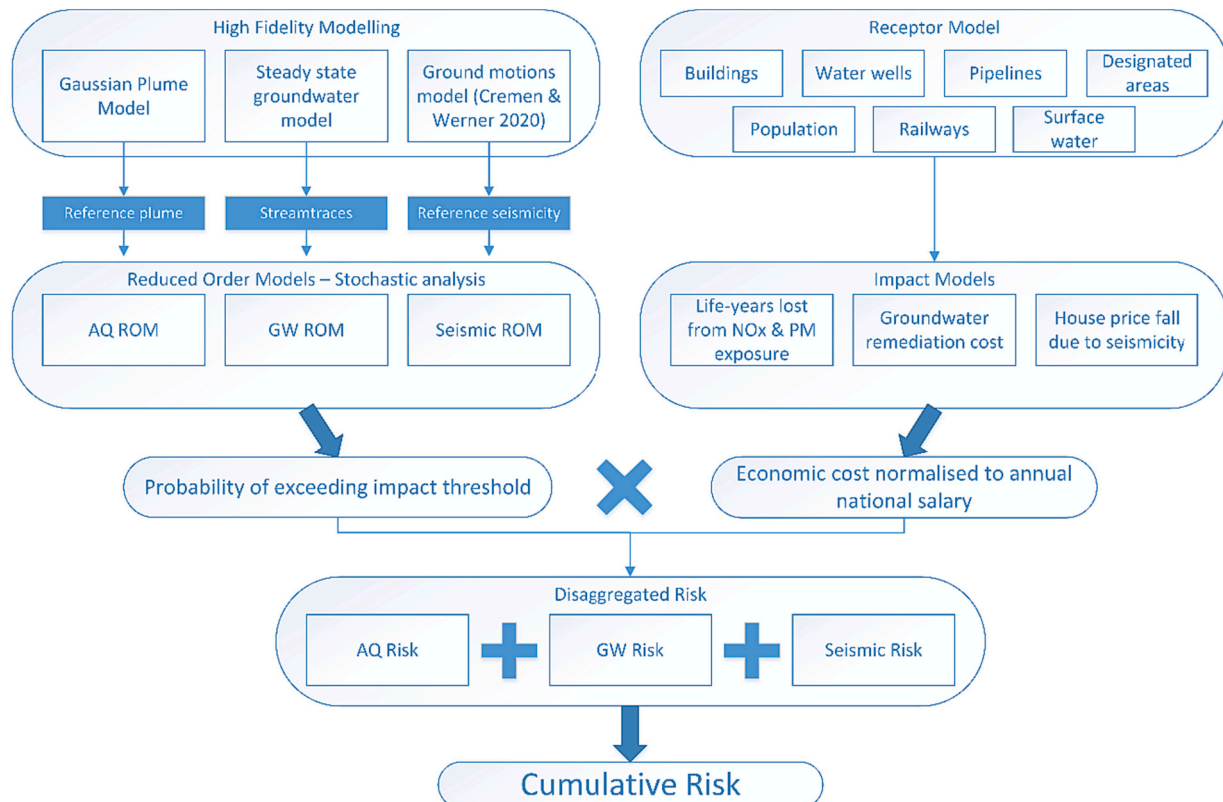

Fig. 3. Flowchart of the risk-assessment methodology; AQ: Air Quality, GW: Groundwater, ROM: Reduced-Order Model; © 2024 University of Edinburgh.

economic cost (Decker, 2018). Given the timescale of groundwater contaminant movement, these costs may increase over time due to changes to energy and processing costs, as well as the impacts of climate change. However, this is the current best estimate for costs incurred. The cost function could be modified to take these temporal changes into account.

Seismicity impacts are based on the change in house prices within 25 km of the well-pad site as a result of felt seismicity from HF operations in the UK (Gibbons et al., 2021). This impact model is chosen because the probability of significant structural damage is low in the modelled scenario and because it provides a simple economic cost metric that can be compared with the other impacts. The house-price metric captures the societal impact of induced seismicity where the physical impact may not lead to a significant risk.

3.4.4. Risk

Risk is calculated as the probability of the impact threshold being exceeded multiplied by the salary-normalised economic cost of exceeding that threshold at each location in the domain for each hazard compartment. We use the UK median annual salary for 2022 of £33,000 (ONS, 2023) as a relatable economic cost of hazards associated with unconventional hydrocarbon exploitation. Where receptors for multiple hazard compartments are present at one location, these calculated risk values are summed to report the cumulative risk. The two main outputs are the spatio-temporal cumulative risk and risk matrices reporting probability of exceeding an impact threshold versus the corresponding economic impact at each location in the modelled domain through time. For the purposes of producing risk matrices, simple "low-", "medium-", or "high-" risk categories were created based on a logarithmic scale. Low risk constitutes probability multiplied by impact less than or equal to the UK median annual salary, medium risk is $1–10\times$, and high risk is $>10\times$.

4. Results

4.1. Air quality and greenhouse-gas emissions

A brief summary of results from atmospheric observations is given using datasets described in Section 3.1 and Table 1. Shaw et al. (2019) presented an atmospheric baseline of GHGs, which observed significant seasonal and diurnal variability, and important relationships with pre-existing local sources of pollution in the areas of the PNR and KMA sites. Existing sources of atmospheric pollutants must be accounted for when assessing the incremental and relative impact of new industrial activities, in this case of HF, on the local environment. A similar baseline assessment was conducted by Lowry et al. (2020), in which local sources of CH_4 pollution were identified and characterised using their $\delta^{13}C$-CH_4 isotopic signature, which varies by source type, and the ratio of ethane to methane (C2/C1), which separates fossil gases (gas pipelines and natural gas generally) from waste and agricultural sources. Baselines were also developed for air-quality pollutants (Ward et al., 2019; Ward et al., 2018b; Ward et al., 2017; Wilde et al., 2023). Collectively, the above body of work demonstrated the importance and utility of multi-year statistical climatologies of atmospheric pollutants, which can inform comparative and quantitative analysis after a local perturbation (HF activity in this case).

By way of example, Fig. 4 shows statistical boxplots by month for CH_4 and CO_2 mixing ratios measured during westerly winds (wind directions between $225°$ and $315°$) between February 2016 and September 2020 at the PNR site. This four-year period spans the base-line, HF-operational and post-operational phases as colour-coded in the figure. The key beneath each month indicates site activities reportedly undertaken on the shale-gas site during each month, referencing publicly available information from the site operator.

Several observations can be drawn from the example in Fig. 4. Firstly, an expected seasonal cycle of atmospheric CH_4 and CO_2 mean mixing ratios is clearly visible. Higher mixing ratios of both CH_4 and CO_2
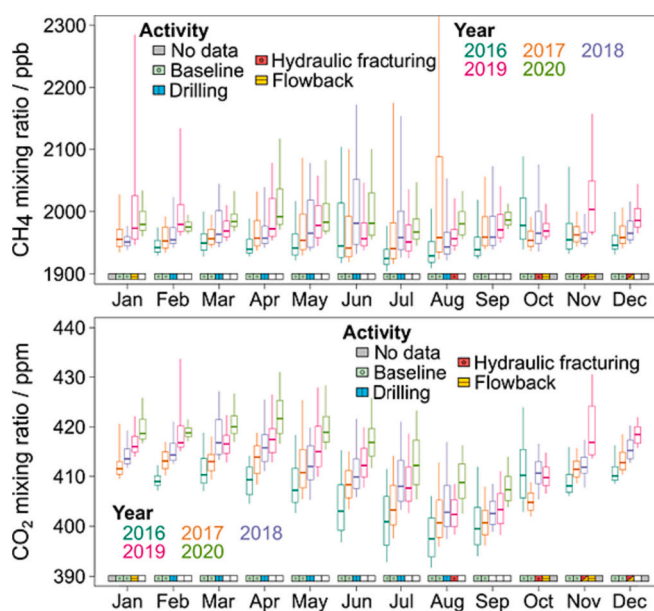

Fig. 4. Boxplots for monthly CH_4 (ppb) and CO_2 (ppm) mixing ratios measured under westerly winds ($270° \pm 45°$) at PNR. Boxplots in different colours represent the different years of data between February 2016 and September 2020. For each boxplot, the thick line represents the monthly median mixing ratio, the outer edges of the box represent the interquartile range, and the upper and lower whiskers extend to the 10th and 90th percentile values respectively. The coloured rectangles below the boxplots provide an indication of the reported activities taking place at PNR during each month. A blank rectangle indicates that there were no reported activities; © 2024 University of Manchester.

were generally measured in the winter months (DJF) compared with summer months (JJA), related to well-known seasonality in the balance of sources and sinks of these gases as the northern hemispheric biosphere waxes and wanes.

A general annualised increase in atmospheric CH_4 and CO_2 mean mixing ratios is also visible. These increases are consistent with the globally reported increase in background CH_4 and CO_2 (of approximately 7–10 ppb CH_4/year, and approximately 2–3 ppm CO_2/year (Lan et al., 2023). However, there were several monthly exceptions to the regular year-on-year increases: October 2016, August and September 2017, and June and July 2018 appear to be anomalously high in CH_4 compared to corresponding months in adjacent years. Whilst drilling was taking place in both June and July 2018, the lack of observed enhancement in CH_4 for other months in which drilling occurred implies that drilling (in itself) had little overall significance to monthly CH_4 statistics. The well-drilling phase was not expected to result in significant emissions of either of CH_4 or CO_2.

Whilst drilling operations had little observed effect on CH_4 and CO_2 statistics, albeit on the basis of a limited number of wells drilled, the impact of flowback operations is very clear (Fig. 4). There was a sharp increase in the 90th percentile for CH_4 mixing ratios in January 2019, as well as a clearly observable difference in CH_4 and CO_2 statistics in November 2019 compared to other years. It should be noted that the median CH_4 mixing ratio in January 2019 was consistent with medians for other years, implying that whilst flowback emissions resulted in a greatly expanded range in measured CH_4, the emission event was generally short-lived (i.e. much shorter than the one-month period used for statistical evaluation). Site activity data reported for November 2019 indicated that flowback gas was flared successfully, likely explaining the corresponding increases in CO_2 mixing ratios as well as CH_4 for that month. There was a substantial increase in both the CH_4 and CO_2 mixing ratio 90th percentile values for February 2019 (compared to analogous months), although no flowback was reported for this period by the

operator.

The vehicle surveys (Lowry et al., 2020) identified farms (mainly cow sheds and manure piles) to the north-west and east of PNR site as plume sources of CH_4, particularly when the cows were indoors. Gas pipeline leaks were identified from the south-west to south-east sector, some of which persisted throughout the baseline period while others were repaired during the surveying period. The largest source of CH_4 was a closed but gassing landfill site 2.5 km west-south-west of the PNR well pad. The plume from this source was detected 2 km away from source during a southerly wind in daytime hours. All these sources could likely contribute to enhanced mixing ratios at the drilling and continuous measurement site, depending on wind direction, particularly during overnight inversion conditions, and more so in winter months when the cows are housed. The $\delta^{13}C$-CH_4 signature of -41 ± 1 ‰ and an excess-over-baseline molar C2/C1 ratio of 0.06 (C1/C2 of 17) for fugitive emissions from gas pipes measured by Lowry et al. (2020) characterise the gas as thermogenic and very similar in composition to the Carboniferous gas from the Preese Hall exploration borehole (see Fig. 5).

In terms of local air quality, statistically significant impacts were first observed during a 20-week period of intensive preparation for HF at the KMA site. Purvis et al. (2019) found that concentrations of NO and NO_2 increased by up to three times the baseline during this 'pre-operational' phase. These pollutant increases were attributed to a combination of increased vehicular activity, and the operation of equipment such as diesel generators on-site. Despite this increase relative to the baseline, air quality limits for NO_x were not found to have been exceeded, even close to the well-site, and therefore risk of local residents' exposure to hazardous NO_x was expected to be minimal. However, concentrations of NO_2 would have exceeded the World Health Organization (WHO) annual-average guideline if sustained over the course of a whole year (beyond the 20-week intensive period observed), with potential negative implications for local public health (Wilde et al., 2023). Pre-operational activity was not found to have resulted in increased concentrations of PM or NMHCs but coincided with decreases in O_3 of 29 % compared to baseline. The conclusions of both Purvis et al. (2019) and Wilde et al. (2023) expose an understudied phase of the HF lifecycle: emissions and air-quality implications may arise even before HF drilling begins (i.e. during site preparation).

Observable impacts on GHG concentrations were first observed during exploratory activities at the PNR site, but only after HF had begun (Ward et al., 2020). Considerable enhancements in atmospheric CH_4 were observed when operators used nitrogen gas to clear the fractured well and artificially promote the flow of natural gas. Enhancements of up to seven times the CH_4 background concentration were measured over a period of several days in January 2019. No concurrent enhancements in CO_2 were measured, implying the direct venting of non-combusted natural gas to the atmosphere (e.g. unignited flare emission). Correlated enhancements in NO_x and NMHCs were also observed. Venting of non-combusted natural gas was in breach of the environmental permit in place for HF operations at the time. However, Shaw et al. (2020) concluded that the CH_4 concentrations observed were unlikely to have posed any direct hazard to local residents, or any explosive risk to workers on-site.

Shaw et al. (2020), made use of three independent approaches to quantify the magnitude of the CH_4 emission flux associated with CH_4 venting in January and February 2019, which concluded an estimated peak CH_4 flux from the site of approximately 70 g/s, with a total mass of CH_4 emitted during the event of 4.2 ($\pm$ 1.4) tonnes CH_4. Whilst this mass of CH_4 is extremely small in the context of national emissions (equivalent to the carbon emitted by roughly 140 transatlantic flights), routine use of nitrogen lifts during exploratory HF could represent a large CH_4 source if shale-gas exploitation is scaled proportionally nationally and flares remain similarly non-combusted. Previous estimates of the impact of shale gas have not typically included emissions during exploration, nor emission estimates for nitrogen lift operations, due to a lack of measurements (Stamford and Azapagic, 2014).

The same CH_4 emission event was also observed using UAV-based sampling. Shah et al. (2020b) used a near-field Gaussian plume inversion approach to quantify CH_4 emissions of between 9 and 156 g/s, in agreement (within acceptable uncertainty bounds) with the flux quantification from fixed-site monitoring studies (Shah et al., 2019; Shah et al., 2020a; Shaw et al., 2021).

We also explored the applicability of machine-learning for automated detection of GHG emissions, using the HF emission event as a case study. Shaw et al. (2022) demonstrated the use of two machine-learning tools for interpreting and modelling baseline data. The models were used to forecast 'business-as-usual' CH_4 concentrations, using baseline training data, in which, from the model perspective, HF never occurred. This counterfactual CH_4 dataset was compared against the measured data to detect successfully any anomalous CH_4 concentrations that could be associated with emissions from HF. The same approach was used by Wilde et al. (2023) to compare the 'pre-operational' phase with a 'business-as-usual' scenario from an air-quality perspective. Such tools represent a potential automated alerting system for emission events, so long as adequate baseline data exist to train such models.

In conclusion, the directly observed risk to air quality and human health, via exposure of local residents to harmful pollutants, can be low if the proper regulatory practices are followed. However, increased activity associated with HF (e.g. movement of vehicles, operation of diesel engines) will always lead to increased local concentrations of pollutants. Risk should be managed by continuous atmospheric monitoring and by ensuring that pollutant concentrations fall well within national and international guidelines. Care should be taken to avoid non-combusted flaring activity to reduce climate impacts of SLCPs such as unburnt methane.

HF presents a larger risk to global climate and the goals of international treaties such as the Paris Agreement, or to national targets such as Net Zero. Whilst singular, localised events involving venting of GHGs such as CH_4 may be small in practice, the possibility of multiple events over the lifetime of single (or multiple) HF sites could be significant.

4.2. Groundwater characterisation

One of the key observations arising from monitoring of groundwater chemistry in the Vale of Pickering and Fylde aquifers is the very large range in concentrations of dissolved CH_4. As one of the fundamental indicators of risk from deep subsurface fluid transport and contamination in the context of shale-gas exploration, CH_4 was an important analyte for investigation. Although observed concentrations were mostly low (up to 6 mg/L but mostly <0.1 mg/L) in groundwater from the Quaternary aquifers of both investigated areas, those in groundwater from the Kimmeridge Clay Formation and Corallian Group of the Vale of Pickering ranged up to around 60 mg/L (Fig. S1) (Smedley et al., 2023). High values were in the most strongly reducing, confined, aquifer conditions.

In each area, groundwater molar methane/ethane (C1/C2) ratios and $\delta^{13}C$-CH_4 isotopic compositions were investigated to try to establish the source of the observed CH_4. Isotopic compositions were only measured in samples where dissolved concentrations were sufficiently high for detection (>1 mg/L). The observed compositions illustrate that groundwater CH_4 in the studied aquifers from both areas is overwhelmingly derived by biogenic reactions in situ rather than by transport of thermogenic CH_4 from deep sources (Fig. 5). A minority of groundwater samples with relatively enriched $\delta^{13}C$-CH_4 compositions (-50 to -44 ‰) relative to other groundwaters measured are interpreted as the likely products of anaerobic or aerobic methylotrophic oxidation (Smedley et al., 2023) rather than originating from deeper thermogenic sources. For comparison, Fig. 5 also shows data for free gases from Carboniferous strata in conventional hydrocarbon boreholes from the Vale of Pickering and from Preese Hall shale-gas exploration borehole in Fylde. These gases contrast with the shallow groundwater data in exhibiting a clear thermogenic signature with more enriched
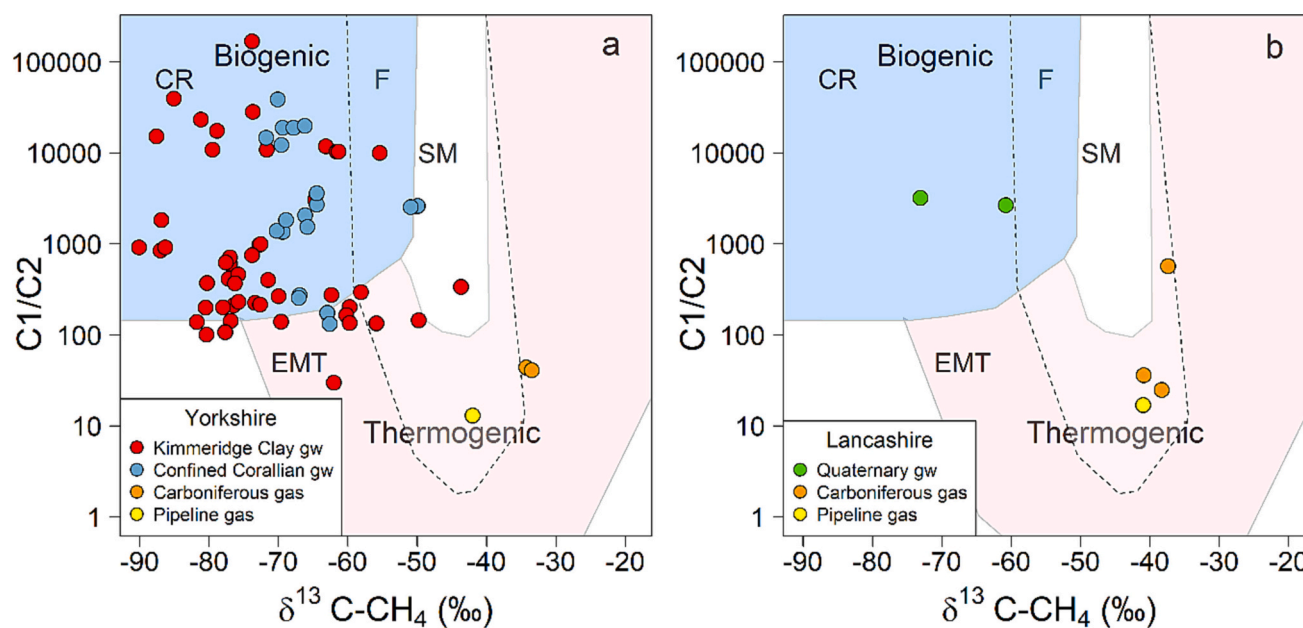
Fig. 5. Molar ratios of methane/ethane (C1/C2) against δ^{13}C-CH$_4$ in groundwater (gw) as well as free gas from Carboniferous hydrocarbon boreholes and atmospheric emissions from gas pipeline leaks in (a) the Vale of Pickering, Yorkshire and (b) Fylde, Lancashire. Carboniferous gas data for the Vale of Pickering are from conventional gas boreholes, those for Fylde are from Preese Hall shale-gas exploration borehole. Data for pipeline gas for each area are from Lowry et al. (2020). Discriminant fields for biogenic and thermogenic methane are also shown, along with fields for CR: CO$_2$ reduction, F: fermentation, SM: secondary microbial (petroleum biodegradation), EMT: early mature thermogenic (fields from Milkov and Etiope, 2018).

δ^{13}C-CH$_4$ (> -45 ‰) and relatively low C1/C2 ratios compared to most of the groundwater data in their respective areas. Data for compositions of atmospheric emissions from gas pipeline leaks are also shown for each area (Lowry et al., 2020). These indicate compositions broadly comparable to the hydrocarbon borehole gases.

Monitored data for Cl and CH$_4$ in groundwater from the Quaternary aquifer of Fylde around and at the PNR site are shown as examples of temporal variability in Fig. S2. As indicators of salinity and hydrocarbon contents respectively, Cl and CH$_4$ are key detectors of any exploration-related impacts over time. Monitoring under baseline conditions, during HF of PNR boreholes 1z and 2, and briefly afterwards, together with statistical modelling of acquired data show that despite the observed variability, especially in concentrations of dissolved CH$_4$, neither analyte shows evidence for change that with confidence can be attributed to HF activities (Smedley et al., 2022).

Monitoring of groundwater from the Fylde network for a range of organic compounds including polycyclic aromatic hydrocarbons, total petroleum hydrocarbons, volatile and semi-volatile organic compounds, as well as acrylamide (the latter investigated since polyacrylamide was reported to be a friction-reducing additive to the frack fluid used at PNR) also did not show evidence of contamination resulting from HF activities. Concentrations of these compounds were overwhelmingly below analytical detection limits throughout the monitoring period (Smedley et al., 2022).

Variations in baseline analyte concentrations in the Vale of Pickering were also investigated by statistical modelling by Ward et al. (2019). The space-time mean for a given analyte (mean analyte concentration across a specified window in space and time as predicted by a statistical model) was computed for 2015–2018 groundwater monitoring data, arbitrarily divided into 'baseline' and 'operational' phases to investigate the consistency between the two. For the analytes Cl, Na, CH$_4$ and NH$_4$, the model results suggested that 20 rounds of groundwater monitoring were insufficient to capture the scale of variation in concentrations and to estimate the baseline model accurately (Ward et al., 2019). Further model simulations indicated that some 30 rounds of baseline monitoring data would be required to capture the variation adequately for the Vale of Pickering case. The findings suggest that characterisation of the baseline and detecting change with confidence requires substantial monitoring effort in cases where groundwater-quality variation is large.

For groundwater modelling, two sets of outputs were produced from the Fylde groundwater-flow model: heads to show that the groundwater model produced reasonable results and particle tracks which fed into the risk-assessment process (Section 4.5). The steady-state groundwater modelling heads showed general flow from the centre of the region to the Fylde coast and rivers (see Fig. S3). Particles were released at the surface, and at depths of 50, 150, 250 and 350 m and were back-tracked to the surface. Fig. S4 shows the frequency distribution for travel time for the model outputs over the depth intervals given. In general, the travel times are long (order of 10s of years) and, as would be expected, the particles released at greater depths have greater median travel times to the surface. The median travel time at the greatest depth (350 m) is 100–200 years, but with a long tail extended to >15,000 years. This demonstrates that the groundwater-flow system has a significant time of travel to the surface and any releases of contaminants from depth would, without preferential pathways, take centuries to millennia to have an impact at the shallow subsurface. It is recognised that if a separate gas phase were present, i.e. two-phase flow system, the travel times of gases to the surface could be faster than for liquid water alone.

4.3. Seismicity

We summarise the results of the forecasting and risk models that were developed using data and methods described in Section 3.3 and Table 1. Cremen and Werner (2020) found a non-negligible exceedance probability (≥ 1 %) of a peak ground velocity (PGV) of 3 mm/s, which is roughly equivalent to the value where vibrations from traffic become perceptible for magnitudes of Mw ≥ 1.6 at distances of up to 2 km. A PGV of 15 mm/s (cosmetic damage for weak structures) becomes non-negligible for Mw ≥ 2.1 at up to 2 km and for Mw ≥ 2.8 at up to 5 km. The cosmetic damage threshold for strong structures (PGV = 50 mm/s) has a negligible exceedance probability for magnitudes of Mw ≤ 3 across all examined distances for any magnitude.

Fig. 6 (left) shows the probability of exceeding different PGV levels for at least one building for different injection volumes. Volumes of
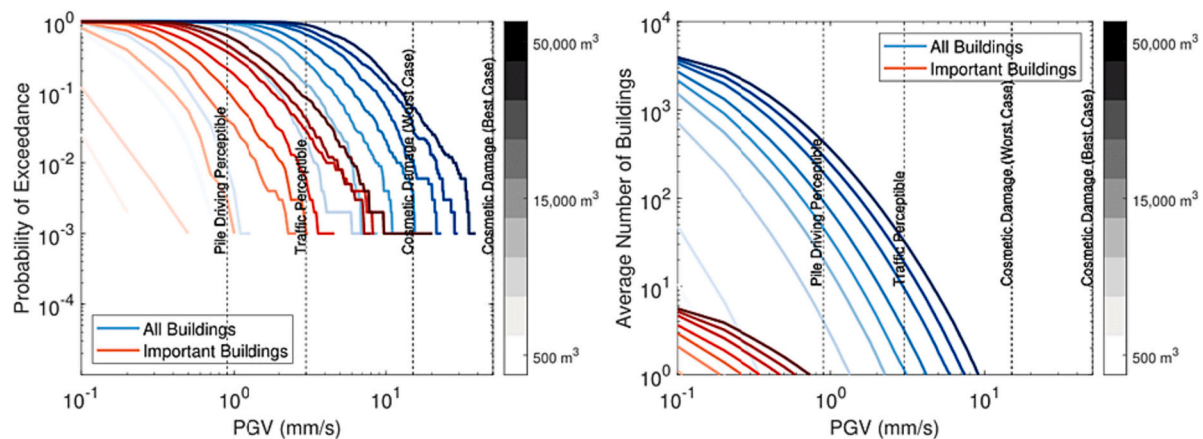
Fig. 6. (Left) the probability of exceeding various PGV levels for at least one building (blue curves) and one important building (red curves) for specific injection volumes of 500, 1000, 5000, 10,000, 15,000, 20,000, 30,000, 40,000 and 50,000 m³. (Right) the average number of buildings (blue curves) and important buildings (red curves) at which various PGV levels are exceeded for volumes of 500, 1000, 5000, 10,000, 15,000, 20,000, 30,000, 40,000 and 50,000 m³. From Cremen and Werner (2020) CC BY 4.0 licence: https://creativecommons.org/licenses/by/4.0.

5000, 10,000, 15,000, 20,000, and 30,000 m³ have approximately a 2 %, 10 %, 30 %, 50 %, and 80 % chance, respectively, of generating ground motions that exceed the level at which traffic-induced vibration becomes perceptible at the location of at least one building in the exposure model. Exceedance probability is lower for important buildings (defined here as hospitals and schools) and is <10 % even for the largest injected volume of 50,000 m³.

The probability of exceeding a PGV where cosmetic damage might occur for at least one weak structure is non-negligible only for the largest injected volumes considered. The probabilities of exceeding the cosmetic damage threshold are 4 % and 7 % for injection volumes of 40,000 and 50,000 m³.

Fig. 6 (right) shows the average number of all buildings (blue curves) and important buildings (red curves) at which various PGV levels are exceeded for different injection volumes. Fewer than one important building is expected to experience shaking that exceeds the lowest of the four considered tolerable risk thresholds for any injected volume analysed. Between 10 and 100 buildings are expected to experience exceedance of the traffic threshold for volumes of 30,000, 40,000 and 50,000 m³. However, fewer than one building is expected to experience cosmetic damage in a worst-case scenario, for any injected volume examined.

Cremen and Werner (2020) noted that the largest contributor to exceeding either threshold is not always the maximum magnitude experienced, particularly for larger volumes of injected fluid, and that intermediate magnitudes are the main contributor to hazard and risk because they occur more frequently than larger magnitudes. However, the scenarios exclude the possibility of larger triggered earthquakes. Cremen and Werner (2020) suggested that this framework facilitates control of the injection volume ahead of time for risk mitigation and can be used to inform policy related to HF-induced seismicity.

Mancini et al. (2021) found that for operations in both PNR-1z and PNR-2, standard ETAS models, optimised using the recorded seismicity, underestimate the observed rates by an order of magnitude during the higher seismicity periods, although they do satisfactorily capture the seismicity decay after the operations or between stages. By contrast, modified ETAS models where the background seismicity rate is proportional to the fluid injection rate to simulate the external forcing due to the pumping of pressurised fluid, provide much better earthquake rate forecasts than standard ETAS models for both PNR-1z and PNR-2. Although the relationship between injection rate and induced seismicity is complex at PNR (Mancini et al., 2019; Mancini et al., 2020), the co-dependency can be approximated linearly and exploited for statistical forecasting purposes (Mancini et al., 2021).

Furthermore, models that are specifically calibrated using data from individual periods of injection perform better than those where the average (bulk) constant of proportionality between seismicity and injection is the rate calculated over the entire period of operations at each well. In particular, the former capture best the high-seismicity rates during periods of injection.

An out-of-sample forecast was also carried out, in which the modified ETAS model was calibrated on PNR-1z and then applied to the PNR-2 data. While the model does not perform as well as the PNR-2-specific models, its estimates are substantially more informative than the standard model, even in periods with high rates.

Mancini et al. (2021) concluded that "operators could provide forecasts during the very early stages of operations using parameters that are either generic or calibrated on adjacent wells", and that "injection-rate-driven statistical forecast models produce informative time-dependent probabilistic seismic rate forecasts." Fig. S5 shows the seismicity rate response during HF operations at PNR (wells PNR-1z and PNR-2), together with the operational parameters: injected volume and injection rate.

4.4. Novel monitoring and evaluation methods

4.4.1. Greenhouse-gas and air-quality monitoring

In addition to the use of novel baseline climatologies (Lowry et al., 2020; Purvis et al., 2019; Shaw et al., 2019), several new techniques were developed during the EQUIPT4RISK project to quantify emission rates (fluxes) of pollutants and to automate the detection of emission events. This included the use of in-situ sensors mounted on unmanned aerial vehicles to map pollution plumes downwind and use of advective transport models and mass balancing to calculate GHG emission rates (Shah et al., 2020b; Shaw et al., 2020; Shaw et al., 2021). A machine-learning tool was also developed and tested for the automated detection of anomalous on-site emissions using baseline data as prior training datasets (Shaw et al., 2022; Wilde et al., 2023). This adds considerable capability in application of statistical techniques for change detection.

4.4.2. Water-quality monitoring

One novel approach to water-quality monitoring has been exemplified in the use of Bayesian hierarchical analysis in assessing impacts. Worrall et al. (2019) proposed the approach to analysis of monitoring data because it is systematic, transparent and provides a probability, with uncertainty, of the nature of any observed data. The probability can be assessed that any environmental impact has or has not happened. This makes use of all available information and so the approach gains

value from the whole monitoring network.

Worrall et al. (2019) proposed that specific electrical conductance (SEC) would be suitable for monitoring the impacts of brine contamination from shale gas and deep subsurface activities on surface-water quality, notwithstanding the probability that salinity poses a smaller contamination risk to the shallow environment than do buoyant hydrocarbon gases. SEC is a frequently-monitored parameter and is an indicator of the total dissolved solids (TDS) content, which in turn is high in shale-gas flowback water in relation to that of fresh water. Rowan et al. (2011) found that flowback fluids from shale-gas formations had TDS concentrations between $^2/_3$–10 times that of seawater (log TDS <4.6) and were larger still relative to freshwater (log TDS ca. 2.6). Thus, SEC (or its related parameters), represents a specific indicator of deep saline groundwater, a direct indicator and a ready indicator (available and inexpensive), albeit not necessarily a sensitive one. Worrall et al. (2019) used a Bayesian hierarchical framework to assess the SEC of English surface water and the scale of spill or leak that could be detected. The Bayesian approach increased sensitivity by an average of 59 %. However, even using the Bayesian framework, the very nature of spills meant that this approach would have only detected continuous chronic leaks to surface water while acute incidents could not have been detected. In response to this, Worrall et al. (2021) used the approach to consider SEC in groundwater, where the longer residence times mean that this could detect a 1 % mix of UK flowback fluids to a 95 % confidence limit. Others have used trace elements such as Br, Li, B and Sr, as well as their respective isotopic compositions, as more sensitive indicators of contamination from deep brines (e.g. Cravotta et al., 2022).

4.4.3. Ground-gas monitoring

Measurement and monitoring of ground gases provides an additional tool for detecting impacts that might arise from subsurface leakage including from shale-gas sources. Measurement may be at fixed points or in survey mode, with continuous-monitoring capability, and can include measurement of gas concentrations or fluxes. Ward et al. (2019) measured soil-gas concentrations from point sources in Fylde and the Vale of Pickering and reported CH_4 ranges of 0–6.5 ppm, mean 1.3 ppm, $n = 357$ and 0–3.3 ppm, mean 1.3 ppm, $n = 448$ respectively. Highest concentrations in the Fylde dataset were recorded at a low-lying, waterlogged site. Most soil-gas concentrations were found to be indistinguishable from local background atmospheric CH_4 concentrations (1.8–2.4 ppm). Methane flux at the sites was also broadly non-detectable (Ward et al., 2019).

As shale gas is derived from rock units that contain abundant organic matter, much regarding associated ground gases can be learned from the monitoring of emissions associated with other organic-rich formations. These include coal and its associated mining activities (Teasdale et al., 2014) and landfills (CL:AIRE, 2021; Wilson et al., 2018). In north-west England, monitoring in boreholes located often in superficial deposits overlying coal-bearing strata has been carried out to identify variations and potential sources of CH_4. Teasdale et al. (2014) reported a study of ground-gas composition measured using the GasClam® that allows for frequent analysis and simultaneous measurement of atmospheric pressure (Fig. S6). Ground gas monitored in a borehole in superficial deposits above Coal Measures (Fig. S6), was found to contain over 30 % (v/v) CH_4, with 10 % (v/v) O_2 and < 5 % (v/v) CO_2, reflecting a complex history of mixing of gas from different sources. Stable C isotopic compositions of CH_4 and CO_2 (δ^{13}C-CH_4, δ^{13}C-CO_2) from monitoring wells in superficial deposits were used to constrain the origin of the CH_4 (Teasdale et al., 2019). The data showed close correspondence with CH_4 known to be derived from coal-bearing rocks in northern England, and clear differences when compared to biogenic gas derived from microbial processes within landfill.

Although the stable-isotope approach is potentially very powerful, it is rarely adopted for routine monitoring of shallow gases including landfill. Instead, the rapid and inexpensive determination, at infrequent intervals (e.g. monthly), of gas concentrations using handheld instruments, relies on the determination of CH_4 irrespective of source. This information is then used to assess risk, including explosion risk, to neighbouring properties.

In the context of shale gas, the experience of landfill-gas monitoring provides valuable knowledge of natural and artificial fluxes of CH_4 from the subsurface to the unsaturated zone. As part of baseline monitoring, rapid sampling using continuous-monitoring instruments, provides comprehensive data for understanding of the dynamics of exchange between soil gases and the atmosphere.

4.5. Risk integration and modelling

Considering the combinations of risks from the different environmental compartments was a key component and ultimate objective of the EQUIPT4RISK project. The development of the integrated risk framework and methodology, described in Section 3.4, captures the cumulative risk from subsurface operations on sensitive human and environmental receptors and defines how the risk changes over temporal and spatial scales. Risk, calculated as the probability of the impact threshold being exceeded multiplied by the UK median-salary-normalised economic cost of exceeding that threshold, is accumulated from the different hazards, to give the cumulative risk at any one location through time.

Fig. 7 illustrates how the temporal evolution of risk varies for each hazard compartment for a 100 × 100 m grid square in Fylde to the southeast of PNR (see Fig. 2a), chosen to be representative of likely receptors. In this case, it shows a modelled scenario in which multiple well pads were developed over a period of 11 years at 5 sites in the study area. The y-axis has a log scale, which facilitates the delineation of low, medium, and high risks, defined by orders of magnitude (green, orange, red) relative to the UK national median annual salary as described in Section
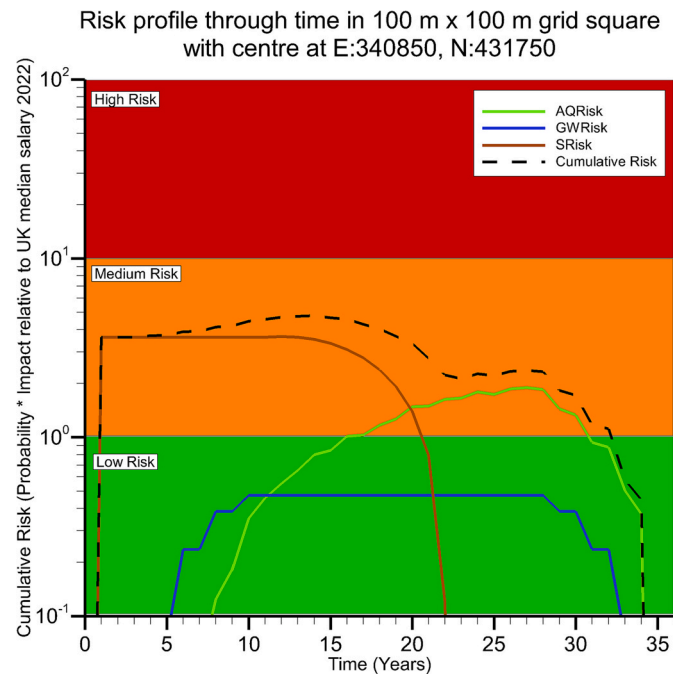

Fig. 7. An example cumulative-risk profile through time at a single grid square in Fylde. Risk is calculated from the probability of exceeding an impact threshold multiplied by the impact of exceeding that threshold relative to the 2022 median annual salary in the UK. Note the log scale on the y axis. Risk profiles relate to air quality (AQ), groundwater quality (GW) and seismicity (S). The risk from each hazard compartment is summed to give the cumulative risk through time (black dashed line). This example is from a scenario where multiple well pads are developed over an 11-year period, with individual lifetimes of 25 years; © 2024 University of Edinburgh.

3.4.4. In this example, each well pad added 10 new wells biannually from Year 1 up to a maximum of 40 wells for each of the five well pads (i. e. 200 wells in total), with each individual well assigned a lifetime of 25 years. Consequently, the spatial distribution of risk from each hazard compartment evolved through time as more wells were developed, produced, and decommissioned at each well pad. The well pad development was offset such that one new well pad came online each year, resulting in a total simulation time of 36 years, and total shale-gas related activity of 35 years. Four of the well pads were sited sufficiently close to each other to demonstrate the evolution of risk where interactions between different well pads were possible. The locations were not representative of real-world well prospects.

HF is active within 25 km of this receptor grid square for the first 11 years, after which the seismic impact model allows for a recovery in house prices (reduction in risk) over the following 10 years. Assuming contaminant release from Year 1 of each well's lifetime, the risk of the groundwater exceeding the national drinking-water limit for Cl is not present until the 6th year of the simulation. The nearest well pad to this receptor grid square (< 200 m) began operation in the 4th year of the simulation and was decommissioned beginning in Year 29. The risk of exceeding the drinking-water limit reduces as the model assumes that successful decommissioning of each well will prevent any further leaks or spills. Despite the proximity of this receptor location to the well pad, the risk of exceeding the air-quality impact threshold from these operations is only present after 8 years of the simulation, or 4 years after the nearest well pad started, indicating that the initial 20 wells on the well pad did not result in significant risk. However, the continued exposure to impacted air quality results in an increase in risk throughout the lifetime of the shale-gas basin, until reducing again as the basin is decommissioned. Fig. 7 illustrates the benefit of considering a holistic approach that combines multiple hazard compartments associated with the development of shale gas, post-shale-gas use or other subsurface geoenergy applications. For example, the cumulative-risk result indicates that this location would have a medium risk for almost the entire duration of shale-gas activities in the area (for this modelled scenario). The risk profiles from each of the individual hazards is quite different both in magnitude and temporal evolution, thus not providing the full picture of the evolution of risk.

5. Discussion

5.1. Establishing the baseline

The various strands of the EQUIPT4RISK study have highlighted the importance of establishing a baseline in environmental conditions to allow quantification with increased confidence of the scale of any new impacts from exploration.

In terms of GHGs and air quality, the project benefited from a world-first and site-specific atmospheric baseline dataset collected for two years prior to HF activity. Without this, it would not have been easy to deconvolve the contribution of HF-specific emissions as a proportion of pre-existing local and regional sources impacting air quality and GHG emissions at each site studied. For example, a dominant atmospheric CH_4 gas source observed at PNR was found to be a nearby dairy farm, which dominated observed atmospheric CH_4 concentrations at all times other than during the non-combusted flaring event in January 2019 (Section 4.1). The dairy farm $\delta^{13}C$-CH_4 isotopic signature was also readily distinguishable from that displayed by thermogenic fossil-fuel sources. The baseline climatology provided useful contextual comparisons, for example that existing agricultural emissions dominated over HF-specific emissions in the local area when considered over the life-cycle of the PNR site. Such comparisons can add meaning in the conveyance of otherwise complex scientific data to the public and other stakeholders. The atmospheric baseline was especially necessary to train machine-learning models used to automate the detection of anomalous emission events (Shaw et al., 2022). Monitoring-site design and

positioning is key to obtaining fit-for-purpose baseline data (as described in Ward et al., 2020).

In terms of groundwater quality, establishing the baseline compositional ranges was necessary to understand the scale of seasonal and longer-term variations ahead of any changes resulting from deep drilling and shale-gas exploration. One of the most significant observations concerning the baseline compositions of Vale of Pickering groundwater from the Kimmeridge Clay and confined Corallian formations has been the regionally high but spatially variable concentrations of dissolved CH_4, as well as detections of C_2H_6 and C_3H_8 in some boreholes (Smedley et al., 2023). The concentrations of CH_4 constitute among the highest observed in UK groundwaters and the maxima are an order of magnitude higher than maxima previously identified from a national survey of CH_4 in groundwater from major aquifers carried out by Bell et al. (2017). The CH_4 stable-isotopic compositions of groundwater from the Jurassic Vale of Pickering aquifers support their overwhelmingly biogenic origin ($\delta^{13}C$-CH_4 mostly < −50 ‰). The C1/C2 ratios vary more widely, with some values below 1000. These have recently been considered as potentially biogenic (Milkov and Etiope, 2018), and observations of C_2H_6 and C_3H_8 also potentially of biogenic origin (Oremland, 1981; Schloemer et al., 2016). Had shale-gas exploration taken place at KMA, correct apportionment of hydrocarbon sources in groundwater would have been much more difficult to assert without the establishment of the baseline conditions beforehand.

Given that methane is also naturally emitted from soils above organic-rich rocks, it is important that baseline measurements of soil-gas emissions be undertaken. Examples from other areas include monitoring emissions from coal occurrences (Teasdale et al., 2014; Teasdale et al., 2019). These are to be at a temporal resolution that allows meteorological effects such as the impact of changing atmospheric pressure on gas transport in the subsurface to be taken into account.

In a low-seismicity environment such as the UK, estimating reliably the background tectonic seismicity rates can be extremely challenging because of the very small number of events that are likely to be recorded in a relatively short time-period. For example, the earthquake activity rate estimated from the last 50 years of instrumentally-recorded earthquakes in the UK, suggests that there are approximately 20 earthquakes with a magnitude of 2 Mw every year. Since the relationship between magnitude and number of earthquakes is exponential, there will be many more small earthquakes, for example, approximately 2000 earthquakes with Mw ≥ 0. If we assume that the probability of occurrence is equal across the whole of the UK, the number in any sub-region scales with the area of that sub-region. In a 30 km by 30 km sub-region, we might expect only 5 earthquakes with Mw ≥ 0 in any year, assuming an area for the UK of approximately 30,000 km². If the activity rate in that sub-region is lower than the UK average, then there will be even fewer earthquakes.

As an alternative, Mosca et al. (2022) developed a national-scale hazard model that captures the probability of different levels of ground shaking for different return periods across the whole UK, and can be considered as a baseline for background tectonic seismicity. This model consists of two parts: one that characterises earthquake occurrence in space and time and another that describes the ground shaking that may result from potential future earthquakes. The results confirm that seismic hazard is generally low in the UK but that the hazard is slightly higher in areas like Wales and north-central England. This largely reflects the higher rates of historical earthquake activity in these regions. The results also show that the hazard is lower than the UK average in both licensed areas: Fylde (licences PEDL165 and EXL269), and the Vale of Pickering (PL80) (see Fig. 2).

5.2. Spatio-temporal variation and magnitude of hazards

The investigation has established differing spatio-temporal hazard profiles and their associated risks for the three environmental compartments. Translation from hazard to risk is strongly dependent on the

impact model, for example, the cumulative risk would be very low if a physical damage model approach to seismicity were used, but seismicity is the largest contributor to risk if a house-price impact model is used. Furthermore, using the house-price impact model reduces the sensitivity of the seismic-risk model to variations in numbers of wells and resulting in a distance-based model that translates the risk beyond the locations where the seismicity is felt. Conversely, the risk to groundwater is captured at discrete boreholes and surface-water locations resulting in the opposite effect from the seismicity by limiting the modelled spatial impact. In this case, a receptor of groundwater-body or aquifer scale may be more appropriate to understand the risk to groundwater abstractions developed in the future, or to groundwater-dependent surface-water ecosystems.

Physical hazard of seismicity is of short duration and is greatest during well development, decaying quickly with time after operations stop, but the impacts may be felt far beyond the spatial and temporal extent of the physical hazard. Furthermore, the impacts of reduced air quality last beyond the duration of the exposure, as health implications caused by chronic exposure are not relieved immediately once operations cease.

The impacts of low-probability, high-impact events should also be considered. For example, while the acute events from the nitrogen-lift emissions were short-lived, they may have lasting impacts (in this case on climate) well beyond the event occurrence.

The differing temporal scales of the three hazard types, i.e. short for air quality and induced seismicity, long for groundwater, underpin and explain the differing responses. While impacts on GHGs, air quality and seismicity were all recognised and recorded around the time of the HF activities at PNR, evidence for impacts on groundwater quality was lacking (Fig. S2). This reflects the slow movement of groundwater in the low-permeability parts of the groundwater system and lack of hydraulic drivers for flow. A potential exception to this would be expedited impacts on groundwater quality due to surface spills and leaks, with a lower probability of local well-integrity failures.

Differing spatial extents of hazards also have a differing impact. Capturing the social risk via house prices extends the impact beyond the location of the actual physical hazard. However, it fails to capture any social benefits that may also be felt from the development of shale gas in any given area, albeit these may be short-lived, including increased jobs and demand for services in the early stages of development.

5.3. Utility of the risk-framework approach

The SPR model is considered an appropriate approach for a defined hazard source from a relatively small area or volume. Examples from this work include induced seismicity from a fracked length of casing or leakage of pollutants from a break/failure in well casing, which can be modelled by identified transport pathways. This approach also works well for other anthropogenic activities where pathways in the environment can be readily defined from site characterisation and conceptual and other modelling approaches. Example anthropogenic activities include those that exploit the deeper subsurface such as mining, a radioactive waste geodisposal facility or similar. The approach is also relevant for reuse of a shale-gas play for storage or disposal. The approach may be less applicable for deep diffuse sources of pollutants where the source is harder to define and characterise. The integrated approach to risk assessment applied for this study is therefore transferable to other point-source hazards or those that have a relatively small footprint.

The risk framework considered risks to air quality, groundwater and seismicity. It is recognised that this does not cover the complete range of potential environmental risks in a shale-gas context. Others include impacts of vehicle movements, noise and risks related to disposal of frack fluids and flowback. Alongside this, infrastructure developments such as gas pipelines to national distribution networks are a requirement that have implications for land ownership and management beyond the

shale-gas area. Whilst these developments were planned, no details are available due to the lack of shale-industry development. These other impacts, along with the climate impact of shale-gas operations, could be assessed in a future, broadened risk framework.

5.4. Future applications

Although shale-gas exploration in the UK has had a faltering history and its further development looks unlikely at the time of writing, the areas of investigation pursued by the EQUIPT4RISK project have broader applications for deep subsurface exploration. These have relevance particularly in the UK's pursuit of its Net-Zero targets and include subsurface technologies such as deep geothermal power, thermal-energy storage, carbon capture and storage and H_2 storage. The methodologies also have application in the developments of coalbed CH_4, enhanced oil recovery and geological disposal of high-and medium-level radioactive waste. All these developments have variable associated costs and benefits, for which application of an analogous risk framework could be appropriate.

Monitoring and modelling methods for investigations of air- and groundwater-quality receptors are directly transferable from those pursued for the shale-gas cases, although the nature of the potential contaminants and their release dynamics will vary. Stable and radiogenic isotopes in air and water have broad applications for discriminating sources, and statistical and machine-learning methodologies have wider applicability in detecting change. For seismicity, subsurface injection and storage (of e.g. CO_2, H_2) may lead to induced seismicity that could pose a risk of damaging ground vibrations or to the integrity of the reservoir itself. Models include operational parameters such as injection rate to estimate the seismic response to injection and can also incorporate the maximum magnitude for tectonic earthquakes at the site of interest. Their generic parameterisation can be calibrated using well-specific information. Monitoring and modelling can also consider ground instability and subsidence resulting from extraction of subsurface fluids.

Seismic forecast models are data-intensive, and their real-time implementation requires detailed earthquake catalogues. This allows models to be refined on different time scales as more data become available. However, out-of-sample models, where the seismicity response to fluid injection is calibrated using data from other sites, also have utility for initial forecasts of seismicity at new sites. A key finding of Cremen and Werner (2020) is that the risk calculations are particularly sensitive to assumptions of the seismicity forecast model used, i.e. whether it limits the cumulative seismic moment released for a given volume or assumes seismicity is consistent with the Gutenberg-Richter distribution for tectonic events. This highlights the importance of understanding the physics to quantify likelihoods of different types of volume-related rupture. Baptie et al. (2022) emphasised that earthquake forecasting remains a scientific challenge for the geoscience community. Maximum expected magnitude, the time scales for the occurrence of large-magnitude earthquakes and the variability of earthquake sequences across the world are all areas of ongoing research. These challenges and issues are shared in natural and induced earthquakes alike.

The depth of analysis in the EQUIPT4RISK project reflects the expertise and infrastructure of a large specialist academic research team and significant time and equipment resources. This was deemed appropriate given the relatively unknown environmental risks of HF activity in a UK context, and because of legitimate public and regulatory concerns. Such effort and scale of analysis could, in principle and with resource, be replicated for future novel industrial use cases, and indeed future HF activity should this ever occur. However, it is reasonable to suggest that such resource and effort may not be possible or appropriate for every new site. There may also be an important question as to who should pay for such research and monitoring activity. Therefore, the lessons learnt in EQUIPT4RISK regarding approaches to monitoring could be adopted more widely, for example as a proportionate toolbox of

monitoring activity and mitigating interventions, following a robust risk assessment and a framework for reduced monitoring. For example, as long as an adequate environmental baseline can be constructed (e.g. from national/regional network monitoring data), and nearby monitors exist to inform the detection of hazardous events, more intensive monitoring (e.g. using UAV, vehicle surveys or screening of air and water for a broader suite of inorganic and organic constituents) could be initiated quickly where needed as long as such a responsive capability is maintained (e.g. by regulators such as the Environment Agency for England). Further, the risk-assessment process presented here occurs within a framework of ISO 31000 which demands regular re-evaluation and modification as changes to the situations occur. Regulatory interventions for various risks and hazards could be developed within that framework, analogous to the traffic-light system that was in place for seismic hazard in the case of HF exploration.

6. Conclusions

We have presented an overview of the scientific findings of the EQUIPT4RISK project, which studied the potential environmental risks of explorative HF activity in the UK. Investigations of air, water and solid-earth seismic compartments in the context of shale-gas exploration have been carried out for the two sites (KMA, Vale of Pickering, Yorkshire and PNR, Fylde, Lancashire) where licences to explore for shale gas were initially granted. The investigations have shown the importance of establishing a baseline to define the pre-development conditions and enable detection of any significant subsequent departures. Investigations of atmospheric GHGs and air quality around PNR and KMA established long-term variability and discrimination of sources. Monitoring also established the scale of emission of non-combusted CH_4 accompanying a nitrogen lift well-cleaning operation at PNR. The study has established the utility of multi-year statistical climatologies of atmospheric pollutants to inform quantitative analysis after a local perturbation.

For groundwater, it was important to identify the existence of high baseline concentrations of dissolved CH_4 as well as detectable ethane and propane in some boreholes. These gases are not ordinarily measured routinely as special sampling arrangements are needed. However, without such a database, it is conceivable that the groundwater hydrocarbon occurrences could and may have been attributed incorrectly to HF and deep sources. In other scenarios, i.e. different industrial operations, other indicators might be critical for defining the baseline against which future change should be compared.

No evidence was seen for any impact of HF at PNR on the chemistry of shallow groundwater locally. This is unsurprising given the curtailed HF activity and the short period of groundwater monitoring subsequently. A much longer period of post-HF groundwater monitoring would have been appropriate if a full-scale HF programme had been conducted. Even then, flow modelling shows that timescales for fluid transport from the deep subsurface to shallow receptors are orders of magnitude longer than those achieved in the groundwater-monitoring programmes.

Probabilistic methods, like those used to quantify risks from tectonic earthquakes can be used to assess risks of induced seismicity. However, there are important differences between how tectonic and induced seismicity evolves in space and time, which requires forecast models that incorporate operational parameters. The specific models developed for PNR show some promise for both assessing risk prior to planned operations and mitigating risks during operations. However, these forecast models are data-intensive, and require detailed earthquake catalogues (high-resolution seismic monitoring, ideally with downhole arrays) for robust calibration. Also, for faults that extend outside the immediate HF zone, the maximum magnitude will be controlled by local geology and tectonics, not by only operational parameters, such as the amount of injected fluid.

Integrated modelling has shown that it is possible to combine risks from multiple different compartments to derive a holistic risk assessment, including different spatial developments and temporal variations, and to provide a final metric for comparison of the different scenarios. It is important to note that conclusions drawn from the cumulative integrated risk example presented in this paper are specific to the small-scale, localised scenario modelled. The risks inherent to a larger-scale HF industry may not simply be linear and cumulative due to site locations and density, population density, and potentially variable site designs and operations.

CRediT authorship contribution statement

P.L. Smedley: Writing – review & editing, Writing – original draft, Project administration, Funding acquisition, Conceptualization. **G. Allen:** Writing – review & editing, Writing – original draft, Funding acquisition, Conceptualization. **B.J. Baptie:** Writing – review & editing, Writing – original draft, Funding acquisition, Conceptualization. **A.P. Fraser-Harris:** Writing – review & editing, Writing – original draft, Software, Formal analysis, Conceptualization. **R.S. Ward:** Writing – review & editing, Funding acquisition, Conceptualization. **R.M. Chambers:** Formal analysis. **S.M.V. Gilfillan:** Writing – review & editing, Funding acquisition, Conceptualization. **J.A. Hall:** Writing – original draft, Conceptualization. **A.G. Hughes:** Writing – review & editing, Writing – original draft, Project administration, Funding acquisition, Conceptualization. **D.A.C. Manning:** Conceptualization. **C. I. McDermott:** Writing – review & editing, Writing – original draft, Funding acquisition, Conceptualization. **S. Nagheli:** Software, Formal analysis. **J.T. Shaw:** Writing – review & editing, Writing – original draft. **M.J. Werner:** Writing – review & editing, Funding acquisition, Conceptualization. **F. Worrall:** Writing – original draft, Funding acquisition, Conceptualization.

Declaration of competing interest

The authors declare that they have no known competing financial interests or personal relationships that could have appeared to influence the work reported in this paper.

Data availability

Data sources are cited in the text

Acknowledgements

Attribution (CC BY) licence to this article.

Appendix A. Supplementary data

Supplementary data to this article can be found online at https://doi.org/10.1016/j.scitotenv.2024.171036.

References

Allen, D.T., 2014. Atmospheric emissions and air quality impacts from natural gas production and use. Annu. Rev. Chem. Biomol. Eng. 5, 55–75. https://doi.org/10.1146/annurev-chembioeng-060713-035938.

Allen, D.T., Torres, V.M., Thomas, J., Sullivan, D.W., Harrison, M., Hendler, A., et al., 2013. Measurements of methane emissions at natural gas production sites in the United States. Proc. Nat. Acad. Sci. USA 110, 17768–17773. https://doi.org/10.1073/pnas.1304880110.

Alvarez, R.A., Pacala, S.W., Winebrake, J.J., Chameides, W.L., Hamburg, S.P., 2012. Greater focus needed on methane leakage from natural gas infrastructure. Proc. Nat. Acad. Sci. USA 109, 6435–6440. https://doi.org/10.1073/pnas.1202407109.

Atkinson, G.M., Eaton, D.W., Ghofrani, H., Walker, D., Cheadle, B., Schultz, R., et al., 2016. Hydraulic fracturing and seismicity in the Western Canada Sedimentary Basin. Seismol. Res. Lett. 87, 631–647. https://doi.org/10.1016/j.jenvrad.2015.07.01610.1785/0220150263.

Atkinson, G.M., Eaton, D.W., Igonin, N., 2020. Developments in understanding seismicity triggered by hydraulic fracturing. Natur. Rev. Earth Environ. 1, 264–277. https://doi.org/10.1038/s43017-020-0049-7.

Babaie Mahani, A., Kao, H., Atkinson, G.M., Assatourians, K., Addo, K., Liu, Y., 2019. Ground-motion characteristics of the 30 November 2018 injection-induced earthquake sequence in Northeast British Columbia. Canada. Seismol. Res. Lett. 90, 1457–1467. https://doi.org/10.1016/j.jenvrad.2015.07.01610.1785/0220190040.

Babaie Mahani, A.S., Ryan, Kao H., Walker, D., Johnson, J., Salas, C., 2017. Fluid injection and seismic activity in the northern Montney play, British Columbia, Canada, with special reference to the 17 august 2015 mw 4.6 induced earthquake. Bull. Seismol. Soc. Am. 107, 542–552. https://doi.org/10.1016/j.jenvrad.2015.07.01610.1785/0120160175.

Baker, J., Bradley, B., Stafford, P., 2021. Seismic Hazard and Risk Analysis. Cambridge University Press, Cambridge.

Baptie, B.J., Luckett, R., Butcher, A., Werner, M.J., 2020. Robust Relationships for Magnitude Conversion of PNR Seismicity Catalogues. Open Report, OR/20/042,. British Geological Survey, Edinburgh, p. 32.

Baptie, B.J., Segou, M., Hough, E., Hennissen, J.A.I., 2022. Recent Scientific Advances in the Understanding of Induced Seismicity from Hydraulic Fracturing of Shales. Report OR/22/050,. British Geological Survey, Nottingham, UK, p. 51.

Bell, R.A., Darling, W.G., Ward, R.S., Basava-Reddi, L., Halwa, L., Manamsa, K., et al., 2017. A baseline survey of dissolved methane in aquifers of Great Britain. Sci. Total Environ. 601, 1803–1813. https://doi.org/10.1016/j.scitotenv.2017.05.191.

Bianchi, M., Scheidegger, J.M., Hughes, A.G., Jackson, C.R., Lee, J.R., Lewis, M.A., et al., 2024. Simulation of national-scale groundwater dynamics in geologically complex aquifer systems: an example from Great Britain. Hydrol. Sci. J. https://doi.org/10.1080/02626667.2024.2320847.

Bommer, J.J., 2022. Earthquake hazard and risk analysis for natural and induced seismicity: towards objective assessments in the face of uncertainty. Bull. Earthq. Eng. 20, 2825–3069. https://doi.org/10.1007/s10518-022-01357-4.

Bradshaw, M., Waite, C., 2017. Learning from Lancashire: exploring the contours of the shale gas conflict in England. Glob. Environ. Chang. 47, 28–36. https://doi.org/10.1016/j.gloenvcha.2017.08.005.

Bradshaw, M., Devine-Wright, P., Evensen, D., King, O., Martin, A., Ryder, S., et al., 2022. 'We're going all out for shale': explaining shale gas energy policy failure in the United Kingdom. Energy Policy 168, 113132. https://doi.org/10.1016/j.enpol.2022.113132.

CL:AIRE, 2021. Good Practice for Risk Assessment for Coal Mine Gas Emissions, CL:AIRE, Reading, UK.

Clarke, H., Eisner, L., Styles, P., Turner, P., 2014. Felt seismicity associated with shale gas hydraulic fracturing: the first documented example in Europe. Geophys. Res. Lett. 41, 8308–8314. https://doi.org/10.1002/2014GL062047.

Clarke, H., Verdon, J.P., Kettlety, T., Baird, A.F., Kendall, J.M., 2019. Real-time imaging, forecasting, and management of human-induced seismicity at Preston new road, Lancashire. England. Seismol. Res. Lett. 90, 1902–1915. https://doi.org/10.1785/0220190110.

COMEAP, 2010. The mortality effects of long-term exposure to particulate air pollution in the United Kingdom, committee on the medical effects of air pollutants. UK 98.

COMEAP, 2018. Associations of long-term average concentrations of nitrogen dioxide with mortality, committee on the medical effects of air pollutants. UK 128.

Connolly, P., 2019. A Simple Gaussian Plume Model for Investigating Air Quality. https://github.com/maul1609/gaussian-plume-model-practical.

Cravotta, C.A., Senior, L.A., Conlon, M.D., 2022. Factors affecting groundwater quality used for domestic supply in Marcellus shale region of north-central and north-East Pennsylvania, USA. Appl. Geochem. 137, 105149 https://doi.org/10.1016/j.apgeochem.2021.105149.

Cremen, G., Werner, M.J., 2020. A novel approach to assessing nuisance risk from seismicity induced by UK shale gas development, with implications for future policy design. Nat. Hazards Earth Syst. Sci. 20, 2701–2719. https://doi.org/10.5194/nhess-20-2701-2020.

Cremen, G., Werner, M.J., Baptie, B.J., 2020. A new procedure for evaluating ground-motion models, with application to hydraulic-fracture-induced seismicity in the United Kingdom. Bull. Seismol. Soc. Am. 110, 2380–2397.

Cremen, G.J., Werner, M.J., Baptie, B.J., 2019. Understanding induced seismicity hazard related to shale gas exploration in the UK. SECED 2019 Proceedings. Society for Earthquake and Civil Engineering Dynamics, p. 10.

Cuadrilla Resources & British Geological Survey, 2021. Homogenised catalogues of microseismicity and pumping data from the PNR-1z and PNR-2 injection wells. In: Centre NGD, editor.

Davies, R.J., Almond, S., Ward, R.S., Jackson, R.B., Adams, C., Worrall, F., et al., 2014. Oil and gas wells and their integrity: implications for shale and unconventional resource exploitation. Mar. Pet. Geol. 56, 239–254.

Decker, C., 2018. Analysis of the Costs of Water Resource Management Options to Enhance Rought Resilience, Final Report for the National Infrastructure Commission. UK, p. 57.

Department for Business Energy & Industrial Strategy, 2013. Regulatory Roadmap: Onshore Oil and Gas Exploration in the UK Regulation and Best Practice. Department for Business Energy & Industrial Strategy, London. https://www.gov.uk/government/publications/regulatory-roadmap-onshore-oil-and-gas-exploration-in-the-uk-regulation-and-best-practice.

Douglas, J., Edwards, B., Convertito, V., Sharma, N., Tramelli, A., Kraaijpoel, D., et al., 2013. Predicting ground motion from induced earthquakes in geothermal areas. Bull. Seismol. Soc. Am. 103, 1875–1897. https://doi.org/10.1785/0120122097.

Edwards, B., Crowley, H., Pinho, R., Bommer, J.J., 2021. Seismic hazard and risk due to induced earthquakes at a shale gas site. Bull. Seismol. Soc. Am. 111, 875–897. https://doi.org/10.1785/0120200234.

Edwards, P.M., Brown, S.S., Roberts, J.M., Ahmadov, R., Banta, R.M., deGouw, J.A., et al., 2014. High winter ozone pollution from carbonyl photolysis in an oil and gas basin. Nature 514, 351–354. https://doi.org/10.1038/nature13767.

Fasola, S.L., Brudzinski, M.R., Skoumal, R.J., Langenkamp, T., Currie, B.S., Smart, K.J., 2019. Hydraulic fracture injection strategy influences the probability of earthquakes in the eagle ford shale play of South Texas. Geophys. Res. Lett. 46, 12958–12967. https://doi.org/10.1029/2019GL085167.

Garcia-Aristizabal, A., Kocot, J., Russo, R., Gasparini, P., 2019. A probabilistic tool for multi-hazard risk analysis using a bow-tie approach: application to environmental risk assessments for geo-resource development projects. Acta Geophys. 67, 385–410. https://doi.org/10.1007/s11600-018-0201-7.

Gibbons, S., Heblich, S., Timmins, C., 2021. Market tremors: shale gas exploration, earthquakes, and their impact on house prices. J. Urban Econ. 122, 103313 https://doi.org/10.1016/j.jue.2020.103313.

Hallo, M., Oprsal, I., Eisner, L., Ali, M.Y., 2014. Prediction of magnitude of the largest potentially induced seismic event. J. Seismol. 18, 421–431. https://doi.org/10.1007/s10950-014-9417-4.

Hammond, P.A., Wen, T., Brantley, S.L., Engelder, T., 2020. Gas well integrity and methane migration: evaluation of published evidence during shale-gas development in the USA. Hydrogeol. J. 28, 1481–1502. https://doi.org/10.1007/s10040-020-02116-y.

Holmgren, J.M., Werner, M.J., 2021. Raspberry shake instruments provide initial ground-motion assessment of the induced seismicity at the united downs deep geothermal power project in Cornwall. United Kingdom. The Seismic Record 1, 27–34. https://doi.org/10.1785/0320210010.

Holmgren, J.M., Kwiatek, G., Werner, M.J., 2023. Nonsystematic rupture directivity of geothermal energy induced microseismicity in Helsinki, Finland. J. Geophys. Res. Solid Earth 128, e2022JB025226. https://doi.org/10.1029/2022JB025226.

Howarth, R., 2015. Methane emissions and climatic warming risk from hydraulic fracturing and shale gas development: implications for policy. Energy Emiss. Control Technol. 3, 45–54. https://doi.org/10.2147/EECT.S61539.

Jenner, S., Lamadrid, A.J., 2013. Shale gas vs. coal: policy implications from environmental impact comparisons of shale gas, conventional gas, and coal on air, water, and land in the United States. Energy Policy 53, 442–453. https://doi.org/10.1016/j.enpol.2012.11.010.

Johnson, C., Bittenbinder, A., Bogaert, B., Dietz, L., Kohler, W., 1995. Earthworm: a flexible approach to seismic network processing. IRIS Newslett. 14, 1–4.

Kasperson, J.X., Kasperson, R.E., 2001. Global Environmental Risk. United Nations University Press and Earthscan Publications Ltd.

Kettley, T., Butcher, A., 2022. Local and moment magnitudes of Preston new road seismicity, 2018-2019. In: Local and Moment Magnitudes of Preston New Road Seismicity, 2018–2019. NERC EDS National Geoscience Data Centre, UK.

Kettlety, T., Verdon, J.P., Werner, M.J., Kendall, J.M., Budge, J., 2019. Investigating the role of elastostatic stress transfer during hydraulic fracturing-induced fault activation. Geophys. J. Int. 217, 1200–1216. https://doi.org/10.1093/gji/ggz080.

Kettlety, T., Verdon, J.P., Werner, M.J., Kendall, J.M., 2020. Stress transfer from opening hydraulic fractures controls the distribution of induced seismicity. Journal of geophysical research: solid. Earth 125. https://doi.org/10.1029/2019JB018794.

Kettlety, T., Verdon, J.P., Butcher, A., Hampson, M., Craddock, L., 2021. High resolution imaging of the ML 2.9 August 2019 Earthquake in Lancashire, United Kingdom, induced by hydraulic fracturing during Preston new road PNR-2 operations. Seismol. Res. Lett. 92, 151–169. https://doi.org/10.1785/0220200187.

Korswagen, P., Longo, M., Meulman, E., Licciardello, L., Sousamli, M., 2019. Damage Sensitivity of Gröningen Masonry – Experimental and Computational Studies (Part 2). C31B69WP0-12,. Delft University of Technology, Delft, The Netherlands, p. 512.

Lan X, Thoning KW, Dlugokencky EJ. Trends in globally-averaged CH_4, N_2O, and SF_6 determined from NOAA Global Monitoring Laboratory measurements, Version 2023–05. 2023. NOAA, 2023.

Lei, X., Wang, Z., Su, J., 2019. The December 2018 ML 5.7 and January 2019 ML 5.3 earthquakes in South Sichuan Basin induced by shale gas hydraulic fracturing. Seismol. Res. Lett. 90, 1099–1110. https://doi.org/10.1785/0220190029.

Llewellyn, G.T., Dorman, F., Westland, J.L., Yoxtheimer, D., Grieve, P., Sowers, T., et al., 2015. Evaluating a groundwater supply contamination incident attributed to Marcellus shale gas development. Proc. Natl. Acad. Sci. USA 112, 6325–6330. https://doi.org/10.1073/pnas.1420279112.

Lowry, D., Fisher, R.E., France, J.L., Coleman, M., Lanoisellé, M., Zazzeri, G., et al., 2020. Environmental baseline monitoring for shale gas development in the UK: identification and geochemical characterisation of local source emissions of methane to atmosphere. Sci. Total Environ. 708, 134600 https://doi.org/10.1016/j.scitotenv.2019.134600.

Mackay, D.J.C., Stone, T.J., 2013. Potential Greenhouse Gas Emissions Associated with Shale Gas Extraction and Use. Department of Energy & Climate Change, London.

Maloney, K.O., Young, J.A., Faulkner, S.P., Hailegiorgis, A., Slonecker, E.T., Milheim, L. E., 2018. A detailed risk assessment of shale gas development on headwater streams in the Pennsylvania portion of the upper Susquehanna River basin, U.S.a. Sci. Total Environ. 610-611, 154–166. https://doi.org/10.1016/j.scitotenv.2017.07.247.

Mancini, S., Segou, M., Werner, M.J., Baptie, B.J., 2019. Statistical modelling of the Preston new road seismicity: towards probabilistic forecasting tools. Commissioned Report CR/19/068, British Geological Survey 38.

Mancini, S., Werner, M.J., Baptie, B.J., Segou, M., 2020. Statistical Modelling and Forecasting of the Preston New Road Seismicity. Commissioned Report CR/20/032,. British Geological Survey, p. 43.

Mancini, S., Werner, M.J., Segou, M., Baptie, B., 2021. Probabilistic forecasting of hydraulic fracturing-induced seismicity using an injection-rate driven ETAS model. Seismol. Res. Lett. 92, 3471–3481. https://doi.org/10.1785/0220200454.

Mansour, M.M., Wang, L., Whiteman, M., Hughes, A.G., 2018. Estimation of spatially distributed groundwater potential recharge for the United Kingdom. Q. J. Eng. Geol. Hydrogeol. 51, 247–263. https://doi.org/10.1144/qjegh2017-051.

Milkov, A.V., Etiope, G., 2018. Revised genetic diagrams for natural gases based on a global dataset of >20,000 samples. Org. Geochem. 125, 109–120. https://doi.org/10.1016/j.orggeochem.2018.09.002.

Molofsky, L.J., Connor, J.A., Wylie, A.S., Wagner, T., Farhat, S.K., 2013. Evaluation of methane sources in groundwater in northeastern Pennsylvania. Ground Water 51, 333–349. https://doi.org/10.1111/gwat.12056.

Morris, B., Medyckyj-Scott, D., Burnhill, P., 2000. EDINA Digimap: new developments in the internet mapping and data service for the UK higher education community. LIBER Q. 10, 445–453.

Mosca, I., Sargeant, S., Baptie, B., Musson, R.M.W., Pharoah, T.C., 2022. The 2020 national seismic hazard model for the United Kingdom. Bull. Earthq. Eng. 20, 633–675. https://doi.org/10.1007/s10518-021-01281-z.

Nisbet, E.G., Manning, M.R., Dlugokencky, E.J., Fisher, R.E., Lowry, D., Michel, S.E., et al., 2019. Very strong atmospheric methane growth in the 4 years 2014–2017: implications for the Paris agreement. Global Biogeochem. Cycles 33, 318–342. https://doi.org/10.1029/2018GB006009.

Nisbet, E.G., Fisher, R.E., Lowry, D., France, J.L., Allen, G., Bakkaloglu, S., et al., 2020. Methane mitigation: methods to reduce emissions, on the path to the Paris agreement. Rev. Geophys. 58, e2019RG000675 https://doi.org/10.1029/2019RG000675.

Ogata, Y., 1988. Statistical models for earthquake occurrences and residual analysis for point processes. J. Am. Stat. Assoc. 83, 9–27. https://doi.org/10.1080/01621459.1988.10478560.

Oil & Gas Authority, 2019. Summary report of the scientific analysis of the data gathered from Cuadrilla's PNR2 hydraulic fracturing operations at Preston new road. Oil & Gas Authority, now North Sea Transition Authority 12.

ONS, 2023. Average household income, UK: financial year ending 2022. Stat. Bull. Office for National Statistics, UK, 2023 https://www.ons.gov.uk/peoplepopulationandcommunity/personalandhouseholdfinances/incomeandwealth/bulletins/householddisposableincomeandinequality/financialyearending2022.

Orak, N.H., Reeder, M., Pekney, N.J., 2021. Identifying and quantifying source contributions of air quality contaminants during unconventional shale gas extraction. Atmos. Chem. Phys. 21, 4729–4739. https://doi.org/10.5194/acp-21-4729-2021.

Oremland, R.S., 1981. Microbial formation of ethane in anoxic estuarine sediments. Appl. Environ. Microbiol. 42, 122–129. https://doi.org/10.1128/aem.42.1.122-129.1981.

Osborn, S.G., Vengosh, A., Warner, N.R., Jackson, R.B., 2011. Methane contamination of drinking water accompanying gas-well drilling and hydraulic fracturing. Proc. Natl. Acad. Sci. USA 108, 8172–8176. https://doi.org/10.1073/pnas.1100682108.

Pawar, R.J., Bromhal, G.S., Chu, S., Dilmore, R.M., Oldenburg, C.M., Stauffer, P.H., et al., 2016. The National Risk Assessment Partnership's integrated assessment model for carbon storage: a tool to support decision making amidst uncertainty. Int. J. Greenh. Gas Control 52, 175–189. https://doi.org/10.1016/j.ijggc.2016.06.015.

Purvis, R.M., Lewis, A.C., Hopkins, J.R., Wilde, S.E., Dunmore, R.E., Allen, G., et al., 2019. Effects of 'pre-fracking' operations on ambient air quality at a shale gas exploration site in rural North Yorkshire. England. Sci. Total Environ. 673, 445–454. https://doi.org/10.1016/j.scitotenv.2019.04.077.

Rowan EL, Engle MA, Kirby CS, Kraemer TF. Radium content of oil- and gas-field produced waters in the northern Appalachian Basin (USA) — summary and discussion of data. U.S. Geological Survey scientific investigations Report 2011–5135, 2011, pp. 31.

Schloemer, S., Elbracht, J., Blumenberg, M., Illing, C.J., 2016. Distribution and origin of dissolved methane, ethane and propane in shallow groundwater of Lower Saxony. Germany. Appl. Geochem. 67, 118–132. https://doi.org/10.1016/j.apgeochem.2016.02.005.

Schultz, R., Stern, V., Novakovic, M., Atkinson, G., Gu, Y.J., 2015. Hydraulic fracturing and the crooked Lake sequences: insights gleaned from regional seismic networks. Geophys. Res. Lett. 42, 2750–2758. https://doi.org/10.1002/2015GL063455.

Schultz, R., Wang, R., Gu, Y.J., Haug, K., Atkinson, G., 2017. A seismological overview of the induced earthquakes in the Duvernay play near Fox Creek, Alberta. J. Geophys. Res. Solid Earth 122, 492–505. https://doi.org/10.1002/2016JB013570.

Schultz, R., Atkinson, G., Eaton, D.W., Gu, Y.J., Kao, H., 2018. Hydraulic fracturing volume is associated with induced earthquake productivity in the Duvernay play. Science 359, 304–308. https://doi.org/10.1126/science.aao0159.

Schultz, R., Quitoriano, V., Wald, D.J., Beroza, G.C., 2021. Quantifying nuisance ground motion thresholds for induced earthquakes. Earthquake Spectra 37, 789–802. https://doi.org/10.1177/8755293020988025.

Shah, A., Allen, G., Pitt, J.R., Ricketts, H., Williams, P.I., Helmore, J., et al., 2019. A near-field Gaussian plume inversion flux quantification method, applied to unmanned aerial vehicle sampling. Atmosphere 10, 396.

Shah, A., Pitt, J.R., Ricketts, H., Leen, J.B., Williams, P.I., Kabbabe, K., et al., 2020a. Testing the near-field Gaussian plume inversion flux quantification technique using unmanned aerial vehicle sampling. Atmos. Meas. Tech. 13, 1467–1484. https://doi.org/10.5194/amt-13-1467-2020.

Shah, A., Ricketts, H., Pitt, J.R., Shaw, J.T., Kabbabe, K., Leen, J.B., et al., 2020b. Unmanned aerial vehicle observations of cold venting from exploratory hydraulic fracturing in the United Kingdom. Environ. Res. Commun. 2, 021003 https://doi.org/10.1088/2515-7620/ab716d.

Shaw, J.T., Allen, G., Pitt, J., Mead, M.I., Purvis, R.M., Dunmore, R., et al., 2019. A baseline of atmospheric greenhouse gases for prospective UK shale gas sites. Sci. Total Environ. 684, 1–13. https://doi.org/10.1016/j.scitotenv.2019.05.266.

Shaw, J.T., Allen, G., Pitt, J., Shah, A., Wilde, S., Stamford, L., et al., 2020. Methane flux from flowback operations at a shale gas site. J. Air Waste Manage. Assoc. 70, 1324–1339. https://doi.org/10.1080/10962247.2020.1811800.

Shaw, J.T., Shah, A., Yong, H., Allen, G., 2021. Methods for quantifying methane emissions using unmanned aerial vehicles: a review. Philos. Trans. R. Soc. A Math. Phys. Eng. Sci. 379, 20200450. https://doi.org/10.1098/rsta.2020.0450.

Shaw, J.T., Allen, G., Topping, D., Grange, S.K., Barker, P., Pitt, J., et al., 2022. A case study application of machine-learning for the detection of greenhouse gas emission sources. Atmos. Pollut. Res. 13, 101563 https://doi.org/10.1016/j.apr.2022.101563.

Smedley, P.L., Ward, R.S., Allen, G., Baptie, B.J., Darakchieva, Z., Jones, D.G., et al., 2015. Site Selection Strategy for Environmental Monitoring in Connection with Shale-Gas Exploration: Vale of Pickering, Yorkshire and Fylde, Lancashire. Open Report OR/15/067,. British Geological Survey, Keyworth, UK.

Smedley, P.L., Shaw, J.T., Allen, G., Crewdson, E., 2022. Environmental Monitoring in the Fylde, Lancashire. Phase 6 Final Report. Open Report OR/22/007,. British Geological Survey, Keyworth, UK.

Smedley, P.L., Bearcock, J.M., Ward, R.S., Crewdson, E., Bowes, M.J., Darling, W.G., et al., 2023. Monitoring of methane in groundwater from the Vale of Pickering, UK: temporal variability and source discrimination. Chem. Geol. 636, 121640 https://doi.org/10.1016/j.chemgeo.2023.121640.

Soeder, D.J., Sharma, S., Pekney, N., Hopkinson, L., Dilmore, R., Kutchko, B., et al., 2014. An approach for assessing engineering risk from shale gas wells in the United States. Int. J. Coal Geol. 126, 4–19. https://doi.org/10.1016/j.coal.2014.01.004.

Stamford, L., Azapagic, A., 2014. Life cycle environmental impacts of UK shale gas. Appl. Energy 134, 506–518. https://doi.org/10.1016/j.apenergy.2014.08.063.

Teasdale, C.J., Hall, J.A., Martin, J.P., Manning, D.A.C., 2014. Ground gas monitoring: implications for hydraulic fracturing and CO2 storage. Environ. Sci. Technol. 48, 13610–13616. https://doi.org/10.1021/es502528c.

Teasdale, C.J., Hall, J.A., Martin, J.P., Manning, D.A.C., 2019. Discriminating methane sources in ground gas emissions in NW England. Q. J. Eng. Geol. Hydrogeol. 52, 110–122. https://doi.org/10.1144/qjegh2018-083.

The Royal Society and The Royal Academy of Engineering, 2012. Shale Gas Extraction in the UK: A Review of Hydraulic Fracturing. The Royal Society and The Royal Academy of Engineering, London.

UK Govt, 2023. Air quality appraisal: impact pathways approach. 2023. UK government, UK. https://www.gov.uk/government/publications/assess-the-impact-of-air-quality/air-quality-appraisal-impact-pathways-approach.

Vasylkivska, V., Dilmore, R., Lackey, G., Zhang, Y., King, S., Bacon, D., et al., 2021. NRAP-open-IAM: a flexible open-source integrated-assessment-model for geologic carbon storage risk assessment and management. Environ. Model Softw. 143, 105114 https://doi.org/10.1016/j.envsoft.2021.105114.

Verdon, J.P., Kendall, J.-M., Butcher, A., Luckett, R., Baptie, B.J., 2017. Seismicity induced by longwall coal mining at the Thoresby colliery, Nottinghamshire, U.K. Geophys. J. Int. 212, 942–954. https://doi.org/10.1093/gji/ggx465.

Walters, K., Jacobson, J., Kroening, Z., Pierce, C., 2015. PM2.5 airborne particulates near frac sand operations. J. Environ. Health 78, 8–12.

Ward, R.S., Smedley, P.L., Allen, G., Baptie, B.J., Darakchieva, Z., Horleston, A., et al., 2017. Environmental Baseline Monitoring Project. Phase II - final report. Open Report,. OR/17/049, British Geological Survey, Keyworth, UK.

Ward, R.S., Allen, G., Baptie, B.J., Bateson, L., Bell, R.A., Butcher, A.S., et al., 2018a. Preliminary Assessment of the Environmental Baseline in the Fylde, Lancashire. Open Report OR/18/020, Nottingham, UK.

Ward, R.S., Smedley, P.L., Allen, G., Baptie, B.J., Cave, M.R., Daraktchieva, Z., et al., 2018b. Environmental baseline monitoring. Phase III final report (2017-2018). Open Report OR/18/026,. British Geological Survey, Nottingham, UK.

Ward, R.S., Smedley, P.L., Allen, G., Baptie, B.J., Barkwith, A.K.A.P., Bateson, L., et al., 2019. Environmental monitoring: phase 4 final report (April 2018–March 2019). Open Report OR/19/044, Nottingham, UK.

Ward, R.S., Rivett, M.O., Smedley, P.L., Allen, G., Lewis, A., Purvis, R.M., et al., 2020. Recommendations for Environmental Baseline Monitoring in Areas of Shale Gas Development. Open Report OR/18/043, Nottingham, UK.

Warneke, C., Geiger, F., Edwards, P.M., Dube, W., Pétron, G., Kofler, J., et al., 2014. Volatile organic compound emissions from the oil and natural gas industry in the Uintah Basin, Utah: oil and gas well pad emissions compared to ambient air composition. Atmos. Chem. Phys. 14, 10977–10988. https://doi.org/10.5194/acp-14-10977-2014.

Whitelaw, P., Uguna, C.N., Stevens, L.A., Meredith, W., Snape, C.E., Vane, C.H., et al., 2019. Shale gas reserve evaluation by laboratory pyrolysis and gas holding capacity consistent with field data. Nat. Commun. 10, 3659. https://doi.org/10.1038/s41467-019-11653-4.

Wilde, S.E., Hopkins, J.R., Lewis, A.C., Dunmore, R.E., Allen, G., Pitt, J.R., et al., 2023. The air quality impacts of pre-operational hydraulic fracturing activities. Sci. Total Environ. 858, 159702 https://doi.org/10.1016/j.scitotenv.2022.159702.

Wilson, S., Collins, F., Lavery, R., 2018. Using ternary plots for interpretation of ground gas monitoring results. Ground Gas Information Sheet No 1. Paper 1.0 30/7/2018, Ambisense and EPG Limited, p. 9.

Worrall, F., Wade, A.J., Davies, R.J., Hart, A., 2019. Setting the baseline for shale gas – establishing effective sentinels for water quality impacts of unconventional hydrocarbon development. J. Hydrol. 571, 516–527. https://doi.org/10.1016/j.jhydrol.2019.01.075.

Worrall, F., Davies, R.J., Hart, A., 2021. Dynamic baselines for the detection of water quality impacts – the case of shale gas development. Environ. Sci.: Processes Impacts 23, 1116–1129. https://doi.org/10.1039/D0EM00440E.